

## The kinematics of multifunctionality: comparisons of biting and swallowing in *Aplysia californica*

David M. Neustadter<sup>1,\*</sup>, Robert L. Herman<sup>2</sup>, Richard F. Drushel<sup>3</sup>, David W. Chestek<sup>1</sup>  
 and Hillel J. Chiel<sup>3,4,1,†</sup>

Departments of <sup>1</sup>Biomedical Engineering, <sup>2</sup>Electrical Engineering and Computer Science, <sup>3</sup>Biology and  
<sup>4</sup>Neurosciences, Case Western Reserve University, Cleveland, OH 44106, USA

\*Present address: 3 Ruth Hamoavia, Apartment 3, Netanya 42756, Israel

†Author for correspondence (e-mail: hjc@case.edu)

Accepted 7 November 2006

### Summary

What are the mechanisms of multifunctionality, i.e. the use of the same peripheral structures for multiple behaviors? We studied this question using the multifunctional feeding apparatus of the marine mollusk *Aplysia californica*, in which the same muscles mediate biting (an attempt to grasp food) and swallowing (ingestion of food). Biting and swallowing responses were compared using magnetic resonance imaging of intact, behaving animals and a three-dimensional kinematic model. Biting is associated with larger amplitude protractions of the grasper (radula/odontophore) than swallowing, and smaller retractions. Larger biting protractions than in swallowing appear to be due to a more anterior position of the grasper as the behavior begins, a larger amplitude contraction of protractor muscle I2, and contraction of the posterior portion of the I1/I3/jaw complex. The posterior

I1/I3/jaw complex may be context-dependent, i.e. its mechanical context changes the direction of the force it exerts. Thus, the posterior of I1/I3 may aid protraction near the peak of biting, whereas the entire I1/I3/jaw complex acts as a retractor during swallowing. In addition, larger amplitude closure of the grasper during swallowing allows an animal to exert more force as it ingests food. These results demonstrate that differential deployment of the periphery can mediate multifunctionality.

Supplementary material available online at  
<http://jeb.biologists.org/cgi/content/full/210/2/238/DC1>

Key words: feeding behavior, biomechanics, kinematics, mollusk, muscular hydrostat.

### Introduction

The same peripheral structure can be used for qualitatively different tasks. Thus, a turtle's leg may be used for scratching regions of the shell (Mortin et al., 1985), for swimming, for stepping, for paddling or for walking (Earhart and Stein, 2000). In crustaceans, the digestive system can process food by grinding, squeezing or filtering it (Harris-Warrick et al., 1992). In many vertebrates, the same limbs are used for both forward and backward locomotion (Ashley-Ross and Lauder, 1997; Ting et al., 1999). The human hand can be used for a remarkable range of tasks, ranging from rapid ballistic movements (as in boxing), to skilled manipulations (as in unscrewing a jar) to a full exercise of its many degrees of freedom (as in piano playing). A hallmark of complex motor systems is the multifunctionality of the periphery, i.e. the ability of the same peripheral structure to execute qualitatively different behaviors (Kelso, 1995).

What are the mechanisms of multifunctionality? Previous work suggests that the many degrees of freedom of the

periphery and reorganizing neural architectures contribute to multifunctionality. Altering the timing or phasing of degrees of freedom makes it possible to rapidly switch among different coordinated movements. For example, changing the timing of monoarticular knee extensor activation contributes to forward swimming as opposed to backpaddling in the turtle (Earhart and Stein, 2000). Changing the activation of unit pattern generators for different joints may be crucial for multi-limbed locomotion in a wide variety of animals, including stick insect and cat (Büschges, 2005).

Studies of neural control in both invertebrates and vertebrates suggest that neural circuitry can control qualitatively different behaviors by reorganizing, i.e. changing connections, or functionally including or excluding neurons, thus rapidly generating different motor synergies (Morton and Chiel, 1994). For example, studies of hypoglossal motor neurons and premotor neurons controlling tongue musculature during breathing, coughing and swallowing in vertebrates such as rats and cats demonstrated that there are shared and unique

patterns of activation of motor neurons during these different behaviors. These observations support the hypothesis that many of the premotor neurons are multifunctional, contributing to the generation of several behaviors (Gestrau et al., 2005). Recently, Berkowitz described spinal interneurons in the turtle whose axon terminal arborizations extend to the ventral horn of the spinal cord, and are rhythmically active in multiple forms of fictive scratching. These observations also suggest that shared interneuronal circuitry is responsible for different motor outputs (Berkowitz, 2005).

Comparing forces and movements underlying similar but qualitatively distinct behaviors is an approach to understanding multifunctionality. For example, a study of movements and EMG associated with forward and backward pedaling in humans demonstrated that the activity of muscles whose biomechanical functions were common in both behaviors were unchanged. In contrast, the activity of muscles whose biomechanical function was different in each behavior was significantly altered by pedaling direction (Ting et al., 1999).

Multifunctionality has primarily been analyzed in musculo-skeletal systems, because it is technically feasible to monitor limb movements and forces during behavior (Biewener, 2002). It has been difficult to analyze multifunctionality in soft-tissue structures. But understanding multifunctionality in soft-tissue structures is likely to be important for deriving general principles, because soft-tissue structures such as tongues, trunks or tentacles [collectively known as muscular hydrostats (Kier and Smith, 1985; van Leeuwen et al., 2000)] have fewer constraints on their degrees of freedom, and generate complex behaviors.

To study multifunctionality in a soft-tissue structure whose nervous system is tractable to detailed experimental analysis, we have focused on qualitatively different feeding responses in the marine mollusk *Aplysia californica*. In *Aplysia*, a 'bite' is an attempt to grasp food (Kupfermann, 1974). As a consequence, bites are associated with large amplitude protractions of the grasper (i.e. the radula/odontophore) past an animal's jaws. If an animal fails to grasp food, it rapidly generates another bite. In contrast, the function of 'swallows' is to convey food that has been successfully grasped into an animal's buccal cavity. As a consequence, swallows are associated with large amplitude retractions of the grasper towards the animal's esophagus (Kupfermann, 1974; Neustadter et al., 2002a; Neustadter et al., 2002b). During the protraction phase of a swallow, the grasper must be moved towards the jaws to grasp more food to ingest, but must not be protracted so far forward that it pushes food out of the buccal cavity. As a consequence, swallows are associated with small amplitude protractions of the grasper (Kupfermann, 1974).

The present study describes how changes in deployment of degrees of freedom of a soft tissue periphery can generate qualitatively different behaviors. Using magnetic resonance (MR) imaging and a three-dimensional kinematic model, we compare muscle movements during biting and swallowing. Our results support the hypothesis that the posterior part of the I1/I3/jaw complex (Fig. 1), previously described as a 'retractor'

(Howells, 1942), may have a context-dependent function and contribute to the larger amplitude protraction observed during biting. The data also suggest that differences in the position of the musculature at the onset of biting are correlated with larger amplitude protractions, and that changes in the closing and retraction of the grasper contribute to the larger amplitude retraction movements observed during swallowing. These changes have important implications for the neural control of multifunctionality.

## Materials and methods

The details of MR imaging of intact, behaving animals, and of creating a three-dimensional kinematic model based on these data, have been presented in detail in several recent papers (Neustadter et al., 2002a; Neustadter et al., 2002b; Neustadter and Chiel, 2004). We will therefore only briefly summarize the MR imaging technique and the kinematic modeling, and focus primarily on aspects of the materials and methods that differ from the previous studies.

### Magnetic resonance imaging

By continuously scanning and interleaving orthogonal images, it was possible to create a rapidly updated reference frame intrinsic to a moving animal. Using this approach, we obtained relatively parallax-free mid-sagittal images of intact, behaving animals. Data were acquired using echo planar imaging with standard two-dimensional Fourier transform reconstruction. The Elscint 2T-Prestige whole-body MRI system was used, with a 15 mT m<sup>-1</sup> maximum gradient strength and 30 mT m<sup>-1</sup> ms<sup>-1</sup> maximum slew rate, allowing 64 encodings with a 1 mm pixel resolution to be acquired in 155 ms. The resolution was 1 mm × 1 mm pixels using a total acquisition matrix of 64 × 128. This spatial resolution is adequate for the buccal masses that were imaged, whose size was on the order 3 cm × 3 cm × 3 cm. The time between repeated acquisitions of the main (mid-sagittal) image was 310 ms, and the time between repeated acquisitions of each orthogonal image (i.e. axial or coronal) was 620 ms.

### Animals and feeding stimuli

The animals used in these studies [*Aplysia californica* (Cooper) obtained from Marinus, Inc., Garden Grove, CA, USA] were the largest that would fit in the holding capsule, and ranged in mass from 400 to 580 g. Analyzable bites were harder to obtain than swallows. As animals swallow a narrow seaweed strip, a seaweed-flavored noodle, or a thin polyethylene tube, they generally do not move their heads and ingest at a regular rate. The low variability in inter-response intervals as animals swallow a narrow seaweed strip is quantified elsewhere (Weiss et al., 1986). In contrast, if an animal does not succeed in grasping food after a bite, it usually moves its head and body in an attempt to better position the radula to grasp food.

We found two ways of reliably inducing bites. First, when animals were initially presented with seaweed-flavored noodles

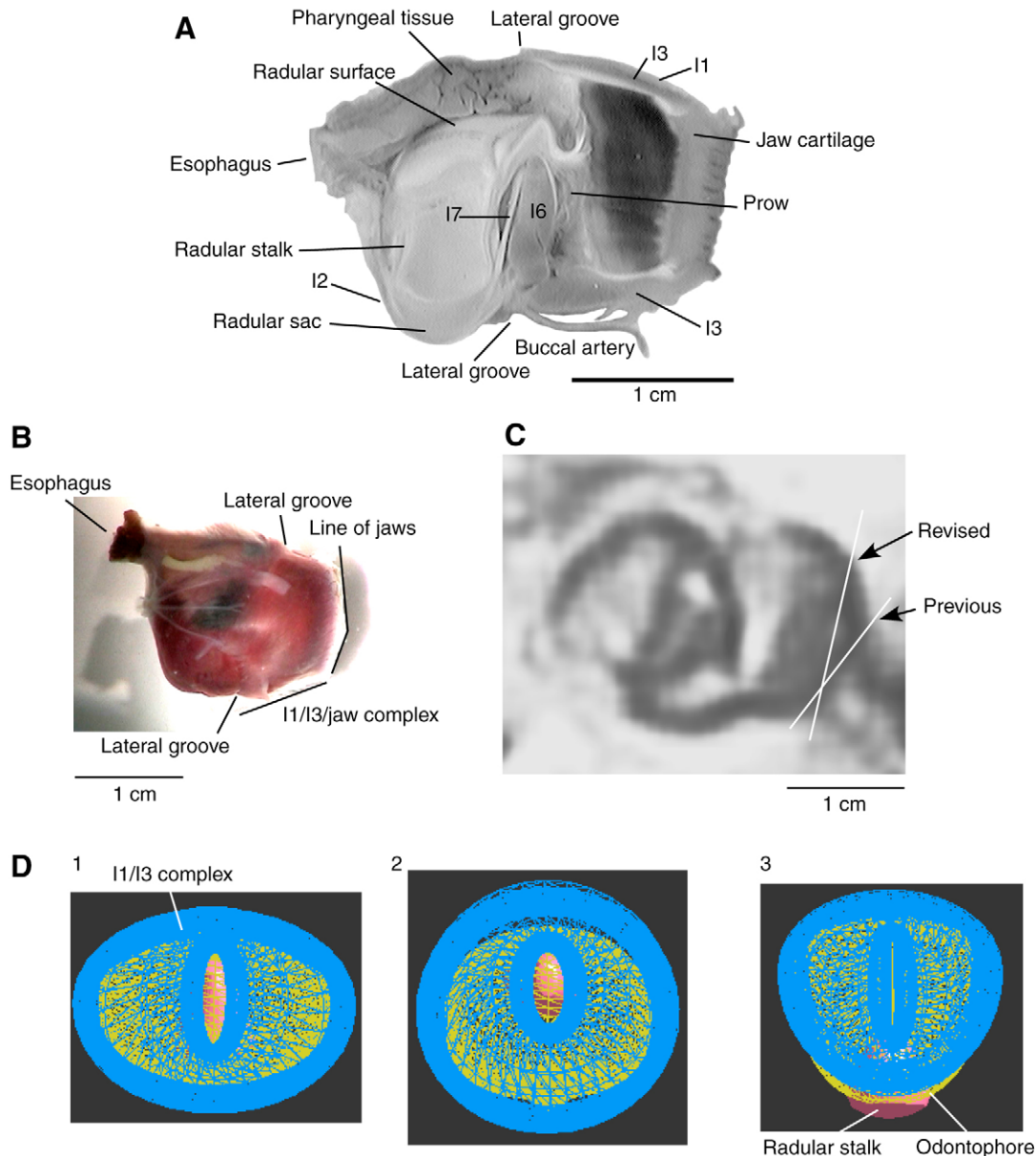


Fig. 1. Anatomy of the buccal mass, and revision of jaw line measurement. (A) Mid-sagittal anatomy of the buccal mass, based on a formaldehyde-fixed hemi-sectioned buccal mass. (B) External oblique view of dissected buccal mass, showing location of jaw line (lines labeled 'Line of jaws'). The I1/I3/jaw complex extends antero-posteriorly from the lateral groove to the jaw line. (C) Line marked 'previous' indicates the jaw line used in previous work (Neustadter et al., 2002a). Line marked 'revised' is drawn from the dorsal point of inflection of the jaw cartilage, which appears as a dark region, to the ventral point of inflection of the jaw cartilage. This more accurately reflects both the external and internal anatomy of the jaw cartilage, which appears in the MR image as a dark region. (D) Antero-posterior views of three-dimensional kinematic model during swallowing using the new jaw line. Blue mesh represents the I1/I3/jaw complex, yellow mesh represents the odontophore, and red solid represents the radular stalk. (1) Transition, (2) protraction, (3) retraction. These views are based on frames 17, 24, and 35, respectively, of sequence 7732-S3. Compare with the bottom row of fig. 11 in Neustadter et al. (Neustadter et al., 2002b). The revised jaw line generates images that are more similar to those observed during swallowing *in vivo*.

(see Neustadter et al., 2002a), they frequently would bite at the noodle at least once or twice before they succeeded in grasping it to swallow it. Second, we constructed a coil of wire connected, *via* a string and a pulley, to a short length of tubing at the front of the capsule into which the animal was placed for imaging. A small piece of seaweed was placed into the short

tube. When a switch was closed, allowing current to flow through the coil, the coil rapidly rotated to align with the MRI's magnetic field, pulling strongly on the string and rapidly retracting the small piece of seaweed held in the tube. Thus, animals were presented with a food stimulus that could be rapidly withdrawn before the animal succeeded in grasping it.

Out of the approximately 12 bites that were relatively parallax-free, we chose to analyze four bites, one from an animal whose swallowing responses were previously analyzed [7725 (Neustadter et al., 2002a)], and three from a second animal. The first and fourth bites were made in response to a seaweed-flavored noodle. The second and third bites were made in response to a rapidly withdrawn piece of seaweed.

#### *Kinematic model*

A kinematic model was used to estimate the full three-dimensional shape of the buccal mass. Although coronal and axial MR images are obtained during feeding to ensure that the mid-sagittal views are free of parallax, these orthogonal images are at lower temporal resolution and have a lower signal-to-noise ratio. Moreover, they captured single slices through the moving buccal mass, and could therefore not be used for full reconstructions.

The kinematic model consists of a model of the radula/odontophore, whose three-dimensional shape is constructed based on parameters extracted from the mid-sagittal MR image, kinematic properties of isolated radula/odontophores, and the assumption that all structures change shape isovolumetrically. It includes a model of the surrounding I3 musculature and an iterative algorithm that positions the I3 model muscles so as to best fit the mid-sagittal MR image of the buccal mass (Neustadter et al., 2002b). Details of the construction of components of the model have been previously described (Neustadter et al., 2002b). We examined the symmetric differences between the coronal MR images and corresponding cross-sections of the model at the peak protraction of biting, and found that they fell within the error tolerances of the results obtained for swallowing [i.e. less than 15%; see fig. 10 in Neustadter et al. (Neustadter et al., 2002b)].

The kinematic model was used to create three-dimensional views of a bite, to estimate the medio-lateral width of the I1/I3/jaw muscle complex, the medio-lateral width of the odontophore, and the length of the I7 muscle. All other data presented in this paper are based on direct measurements of mid-sagittal MR images.

#### *Measurements from MR images*

To extract specific measurements of muscle lengths, and of parameters for the kinematic model, MR images were imported into Paint Shop Pro (version 7.0, JASC Software, Eden Prairie, MN, USA), and the following kinematic measures were drawn on each image in different layers: (1) jaw line, (2) radular stalk outline and radular stalk angle, (3) lateral groove (the borders of the I1/I3/jaw complex dorsally and ventrally), (4) odontophore angle (the angle of the anterior edge of the I6 muscle), (5) an outline of the odontophore, excluding the base of the radular stalk if it protruded below the odontophore, and (6) an outline of the entire buccal mass including the jaw musculature, the odontophore and the radular stalk, but excluding the pharyngeal tissue [fig. 4 (Neustadter et al., 2002a)]. As was done previously, the length of the I2 muscle

was estimated from the posterior portion of the buccal mass outline bounded dorsally and ventrally by the location of the lateral groove, which is the anatomical border of the I2 muscle (Neustadter et al., 2002a). Previous studies showed that these measures were accurate within 5% (Neustadter et al., 2002a).

The only change from the previous measurements was the location of the jaw line. To create a more accurate model of the I1/I3/jaw complex, we have marked its circumference and videorecorded the deformations of its surface in isolated buccal masses during spontaneous and drug-induced movements. Our studies have shown that, at the line of the jaw, the dorso-ventral extent of the jaws does not decrease to the extent suggested by our previous placement of the line of the jaws (Fig. 1A,B). Thus, we have re-analyzed the swallows using a new jaw line placement, which is drawn from the dorsal and ventral inflections of the jaw cartilage (Fig. 1C, line marked 'revised'; note how this follows the anterior margin of the jaw cartilage) rather than from the ventral anterior margin of the dark jaw cartilage region (Fig. 1C, line marked 'previous'). This revision to the position of the line of the jaws had no qualitative impact on any of the conclusions presented in the previous papers on swallowing (Neustadter et al., 2002a; Neustadter et al., 2002b), although the quantitative values of some measures referenced to the jaw line have changed slightly. New views of the front of the feeding apparatus are provided based on the new jaw line measurement (Fig. 1D), which match *in vivo* behavior, and can be compared to the views published previously using the less accurate jaw line measurement [see fig. 11C in Neustadter et al. (Neustadter et al., 2002b)]. All averaged swallowing data shown in this paper are based on the new jaw measurements.

#### *Visualizing fiber directions in the I1/I3/jaw complex*

To visualize the fiber directions in the I1/I3/jaw complex, buccal masses were fixed in 10% v/v formalin in isotonic MgCl<sub>2</sub>, pH 7.5 (Drushel et al., 1998). Hematoxylin (Sigma, St Louis, MO, USA) was mixed with distilled water to create a saturated solution, and then oxidized with sodium iodate (Sigma) to create hematein (a brownish dye), which was applied to the outer surface of the I1/I3/jaw complex. The thin I1 tissue was then dissected away, and the thick bands of the underlying I3 muscle were stained using Fast Green (Sigma). Fibers were then photographed at low power through a stereo dissecting microscope.

#### *Measurement of jaw circumference during biting*

To test the hypothesis that the anterior portion of the I1/I3/jaw complex might exert forces differently than its posterior portion, we measured the most anterior portion of the jaw cartilage during biting. During a significant portion of the biting cycle, it is possible to see the anterior margin of the I1/I3/jaw complex. To measure the circumference of the anterior I1/I3/jaw complex, we placed a digital video camera (ZR10, Canon Inc., Tokyo, Japan) immediately above an animal's mouth, while inducing it to make strong bites by stroking its anterior tentacles and lips with seaweed, and simultaneously applying drops of

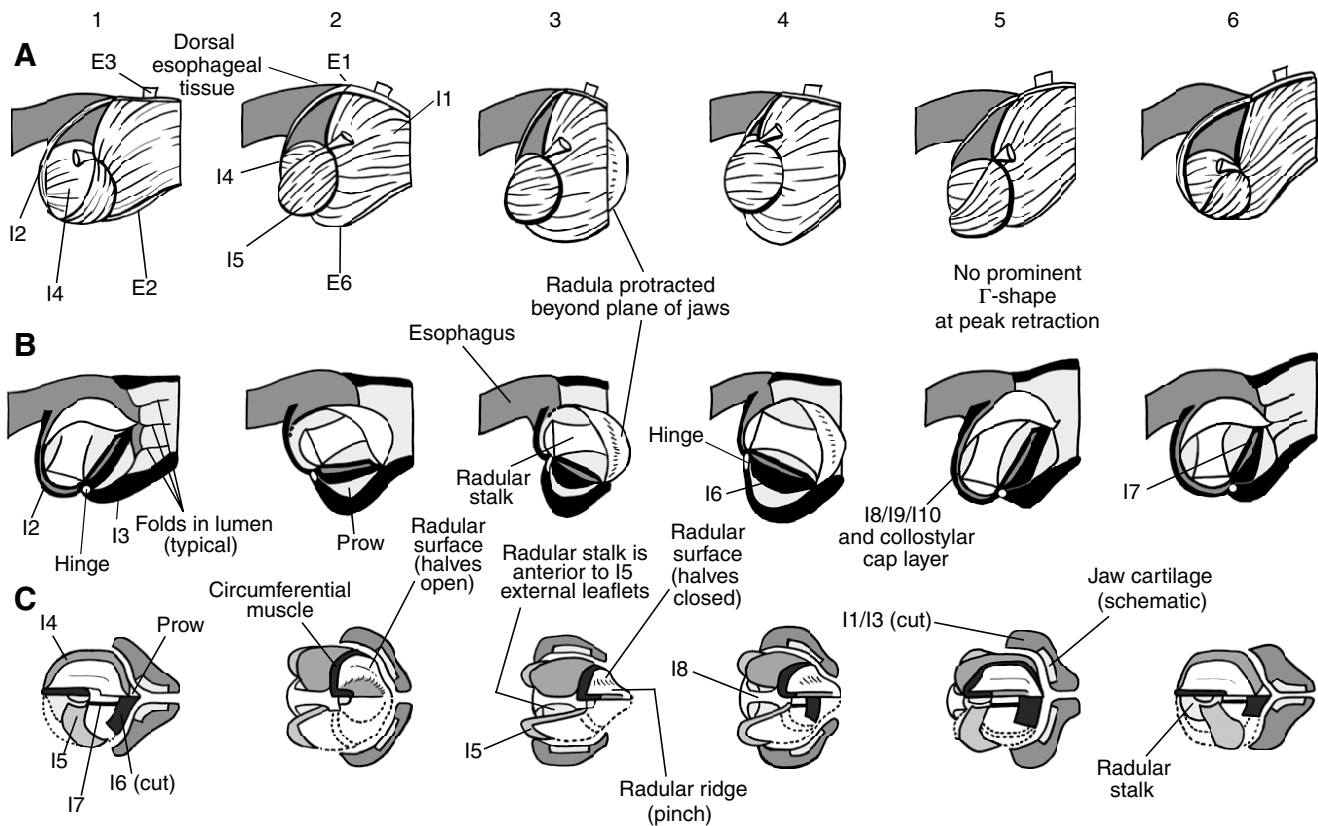


Fig. 2. Schematic summary of the movements of the entire buccal mass during a biting cycle. This summary is based on the data presented in this paper and incorporates observations from *in vivo* high-temporal-resolution MR images in intact, behaving animals as well as high-spatial-resolution MR images of anesthetized buccal masses. Details not visible in the MR images are based on observations of buccal masses or isolated odontophores undergoing pharmacologically induced feeding-like movements, as well as from dissections of fresh and fixed buccal masses. All illustrations are in orthographic projection. (A) Row shows a superficial lateral view of the outer buccal mass. Fiber directions of the thin, overlying I1 muscle are schematically indicated (see Fig. 12A). (B) Row shows a mid-sagittal view. (C) Row shows a dorsal view. The upper half of each panel shows a superficial dorsal view, whereas the lower half shows a view in which the radular surface and the I4 muscles are transparent, revealing the ventral structures beneath them. Columns 1–6 correspond to frames 53, 56, 60, 63, 68, 71 of sequence 3222 (respectively). The circumferential muscle shown in C2 was designated as such by Starmühlner (Starmühlner, 1956). The nomenclature for the other intrinsic muscles (I1 through I10) follows Howells (Howells, 1942) and Evans et al. (Evans et al., 1996), and the nomenclature for the extrinsic muscles (E1–E3 and E6) follows Chiel et al. (Chiel et al., 1986) and Howells (Howells, 1942). Compare with fig. 21 of Neustadter et al. (Neustadter et al., 2002b).

seaweed extract to its lips. Three animals were used for these experiments. We analyzed four bites from one animal that provided the clearest images and showed minimal movement of the plane of the jaws during bites. During the initial phases of protraction, the jaw line is partially obscured by the anterior tentacles, which close prior to protraction [see fig. 2A, first two frames in Morton and Chiel (Morton and Chiel, 1993a); fig. 10C,D in Hurwitz et al. (Hurwitz et al., 1996)], so we measured the jaw cartilage circumference from just before the peak of protraction through jaw closing, during which the jaws are completely visible. Canvas 9.0 (ACD Systems, Miami, FL, USA) was used to trace and measure the circumference of the jaws from digital video images.

#### *Estimating forces on the odontophore from the I1/I3/jaw complex*

Because the anterior portion of the I1/I3/jaw complex

contains folds, it may not exert as much force as the posterior portion of the I1/I3/jaw complex, especially before the peak of protraction. To look at the possible implications of lower forces in the anterior portion of the I1/I3 complex before the folds are fully stretched, we used the three-dimensional kinematic model to compute estimates of the forces that the I1/I3/jaw complex could exert on the odontophore as the odontophore changed position within the I1/I3/jaw complex. To estimate the forces that the different portions of the I1/I3/jaw complex could exert upon the odontophore, the model allowed the ratio of anterior to posterior force to be modified. At each frame of the model, we computed the total force that the I1/I3/jaw complex would exert upon the odontophore if the I3 muscle were contracted with each of four different excitation ratios. We assumed that if a section of the odontophore surface were near a band of the I3 muscle (within a small distance tolerance), then the I3 muscle could apply force to the odontophore over that section.

The force had a magnitude that was proportional to the area of the section that was in contact, and a direction normal to that section. Both the I3 bands and the odontophore were represented as meshes of triangles. The algorithm iterated over each of the triangles representing the odontophore surface, checking to see if a triangle was in contact with part of the I3 muscle. If so, a force was added (as a vector sum) to the total force on the odontophore, proportional in magnitude to the size of the odontophore triangle. Because these studies examined the effects of contracting the muscle, which would cause it to shorten, the forces presented are an overestimate of the actual forces (since, as a muscle shortens, the force it can exert is reduced by its length/tension and force/velocity properties). Thus, these results constitute an upper bound on the forces that the different components of the I1/I3/jaw complex might exert on the radula/odontophore.

#### Data analysis

The feeding cycle was normalized on the basis of the definitions of feeding cycle components from our previous work (Drushel et al., 1997; Drushel et al., 1998; Neustadter et al., 2002a). From the onset of protraction to its peak is designated as  $t_4$ . Peak protraction to peak retraction is designated as  $t_1$ . For swallows, the time from peak retraction to the loss of the shape in which the base of the elongated radula/odontophore extends ventrally along the antero-posterior axis of the buccal mass (termed the  $\Gamma$  shape) is designated as  $t_2$ . Cycle times for swallows were normalized to the sum of these three periods,  $t_4+t_1+t_2$ . In biting, the  $t_4$  period was also observed. However, as we report below, the  $\Gamma$  shape is not observed during bites, although the ventral protrusion of the radular stalk and the posterior rotation of the odontophore (components of the movements that give rise to the  $\Gamma$  shape in swallowing) are observed during the retraction phase of biting. Thus, in biting, the  $t_1$  and  $t_2$  periods blend into one another and are referred to as  $t_1$ . As a consequence, cycle times for bites were normalized to the sum of the periods  $t_4+t_1$ .

To directly compare biting and swallowing on the same scale, we computed our standard reference length, the radular stalk width (RSW). For the first animal (first bite), it was 61 pixels, and for the second animal, it was 59 pixels (second through fourth bite). We found that using these values made no qualitative, and small quantitative differences in the data. Moreover, in the previous study, the RSW for both animals studied was 61. Thus, we chose to report lengths in mm rather than in units of RSW.

After normalizing and averaging, data were smoothed using cubic spline interpolation. Functions for the standard deviation of the data were constructed (Neustadter et al., 2002a; Neustadter et al., 2002b): interpolation functions for each individual normalized data set were subtracted from the interpolation function of the averaged normalized data set. These differences were squared, summed and divided by the number of samples minus 1 (i.e. by  $4-1=3$ ). The square root of the resulting function was taken, creating a standard deviation function. The normalized, averaged data function was plotted, with the standard deviation function added to or subtracted from it. This

indicates the dispersion around each point in the averaged function. Inferences about significant changes in kinematic variables during the swallowing or biting cycle were drawn only if two points on the averaged curve differed by more than two standard deviations. This is a conservative measure of statistical significance, because the appropriate statistic is a difference larger than two standard errors of the mean, obtained by dividing the standard deviation functions by the square root of  $N$ , or by 2 (for  $N=4$ ). All numerical values are reported as mean  $\pm$  standard deviation (s.d.). Statistical significance of numerical differences was determined using Student's  $t$ -test.

As adjuncts to the text, we provide digital movies (in Quick Time format) of one MRI sequence of biting (Movie 1 in supplementary material), showing the second bite analyzed in this paper in sagittal, coronal and axial views, as well as three-dimensional views of this sequence generated by the kinematic model (Movies 2–4 in supplementary material).

#### Results

Using the same musculature, how does an animal generate two functionally distinct behaviors: large amplitude protractions and small amplitude retractions during biting, and small amplitude protractions and large amplitude retractions during swallowing? We examined four specific hypotheses about the differences between the two behaviors.

First, the larger amplitude protractions in biting as compared to swallowing could be due to differences in the positions of the muscles at the onset of each behavior, i.e. at the onset of protraction. We therefore compared the initial positions of the musculature in biting and swallowing.

Second, the grasper opens more widely near the peak of protraction during biting than it does during swallowing, which could be due to the position of the grasper as a whole, or of structures within the grasper. We therefore compared the position of the grasper and changes in its shape and internal structures prior to and at the peak of protraction.

Third, a kinetic model of the buccal mass predicted that the protractor muscle I2 (Fig. 1A, Fig. 2) might become too short in biting to fully protract the radula/odontophore. The kinetic model also predicted that the posterior portion of the I1/I3/jaw muscle (Figs 1, 2) could change function and contribute to protraction (Sutton et al., 2004b). We therefore compared the lengths of I2 and the different regions of the I1/I3/jaw complex in biting and swallowing, and predicted the upper bounds on the net force that the posterior portion of the I1/I3/jaw complex could exert.

Fourth, during swallowing, closure of the grasper and retraction are the power phase, in which the grasper exerts maximum force against seaweed that it is attempting to ingest. We therefore compared closure and retraction of the grasper during biting and swallowing.

#### Overview of biting versus swallowing kinematics

Bites had a similar overall temporal structure to swallows. The duration of the bites that we analyzed was comparable to the duration of the swallows that we studied previously. Bites

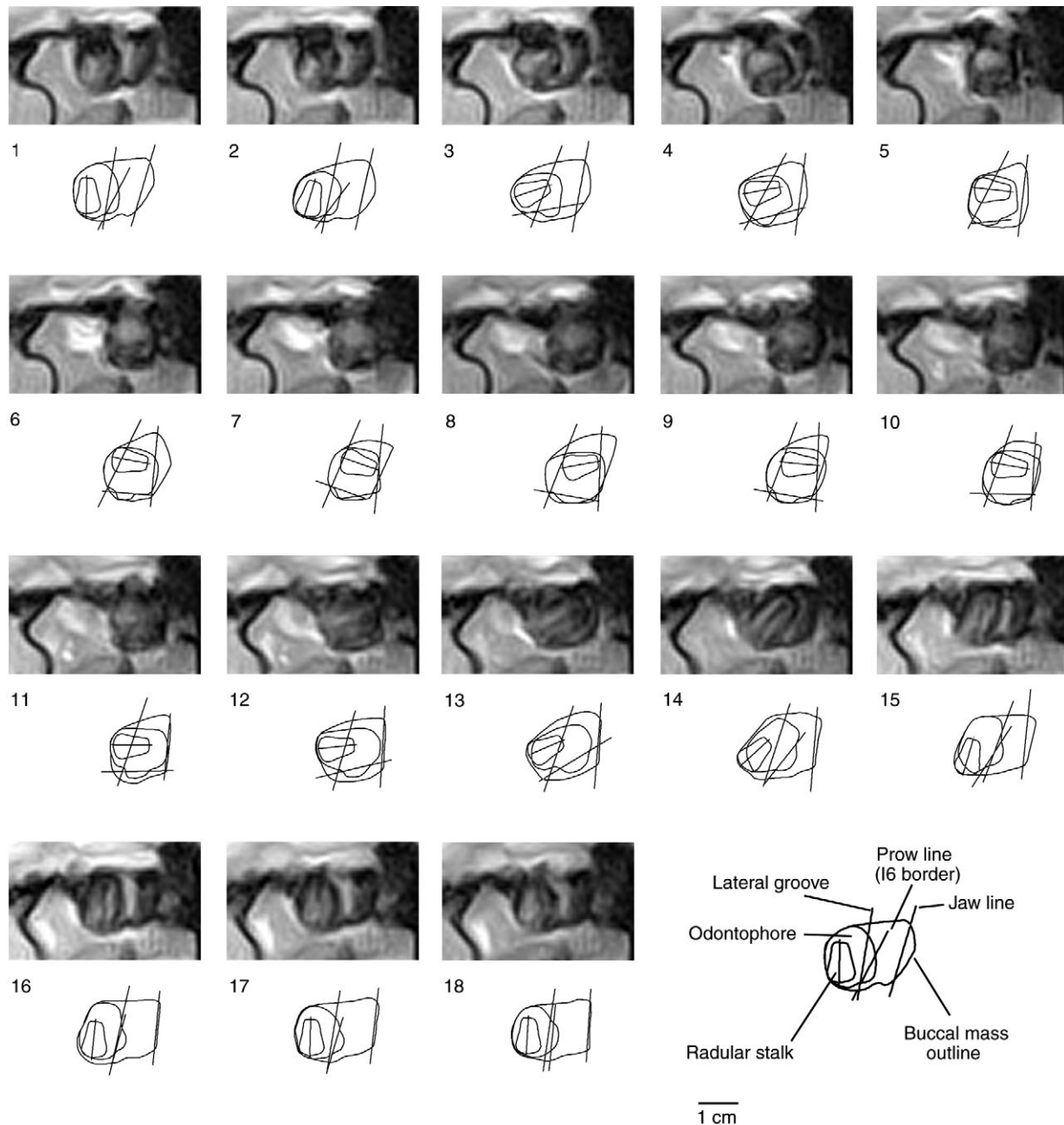


Fig. 3. A sequence of magnetic resonance (MR) images showing biting in response to a rapidly withdrawn piece of seaweed. Frames are acquired in 155 ms and are separated by 310 ms. The high temporal resolution data are shown above the kinematic measures taken from these images (see Materials and methods). This sequence is 3213, frames 26–43.

had a duration of  $5.9 \pm 0.9$  s, whereas swallows had a duration of  $6.4 \pm 0.4$  s [mean  $\pm$  s.d.; swallow durations are for swallows previously reported (Neustadter et al., 2002a; Neustadter et al., 2002b)]. Although the percentage of the cycle devoted to protraction was larger in biting than in swallowing ( $43 \pm 6\%$  for biting *versus*  $37 \pm 8\%$  for swallowing), the difference was not statistically significant.

Despite the temporal similarity, qualitative differences between bites and swallows were apparent from the mid-sagittal MRI images of bites (Fig. 3). The initial position of the

odontophore within the buccal mass just prior to the onset of protraction differed from its initial position in swallowing. The initial length of the anterior portion of I1/I3 was shorter in biting relative to the corresponding initial length for a swallow [compare the dorsal and ventral surface of I3 in Fig. 3, frame 1 of this paper with the same surfaces in fig. 5, frame 1 in Neustadter et al. (Neustadter et al., 2002a)].

At the peak protraction of biting, the anterior portion of the odontophore protruded past the line of the jaws (Fig. 3, frames 7–10); this was never observed during swallowing. At the

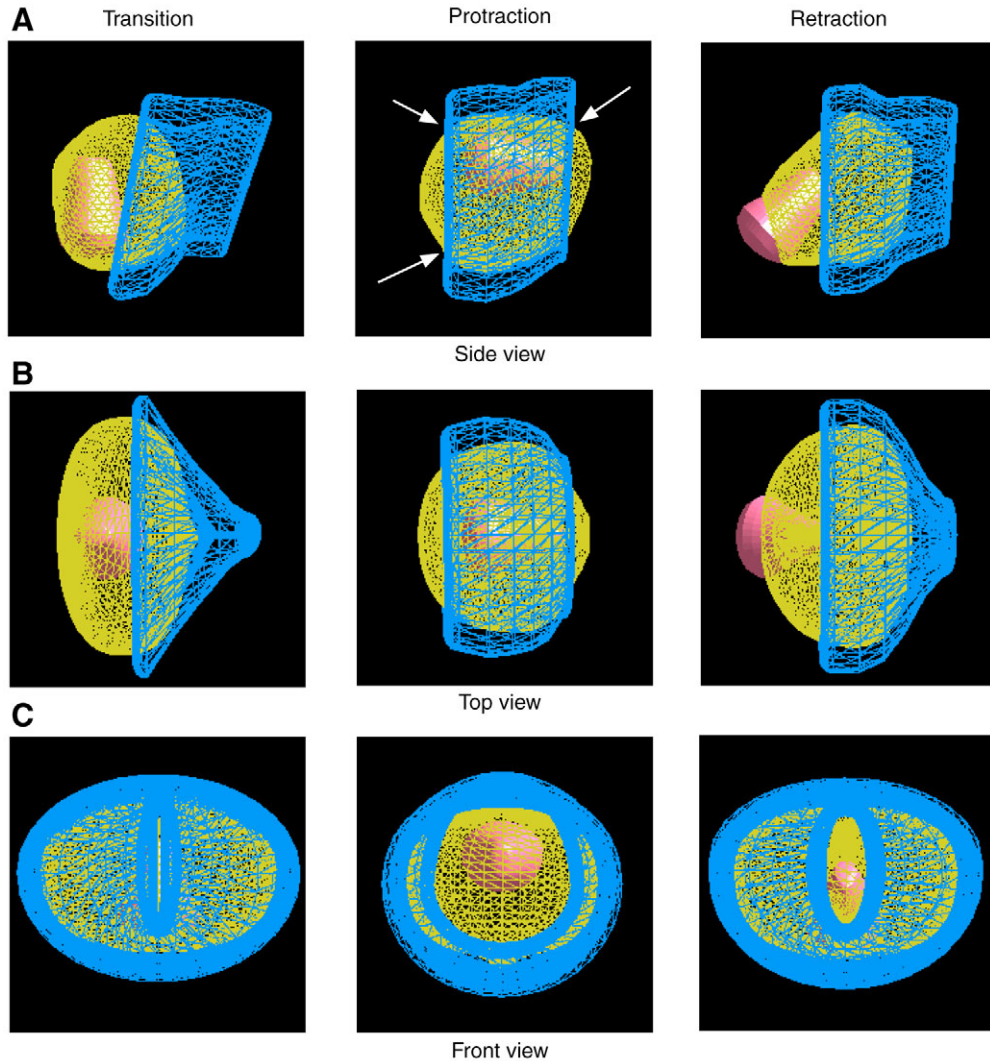


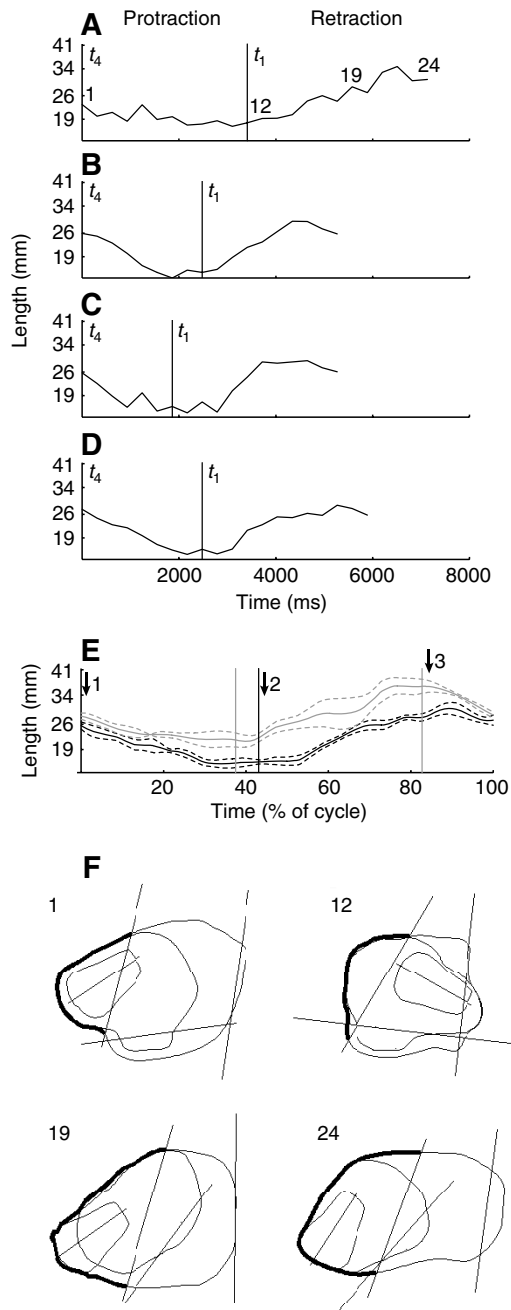
Fig. 4. Three-dimensional kinematic model of the buccal mass during a biting cycle. The 11/13 muscles are shown as a continuous blue mesh, the odontophore is shown as a continuous yellow mesh, and the radular stalk is shown as a red solid. Views are shown in orthographic projection. (A) Right lateral views of transition, protraction and retraction. The central panel shows a side view of protraction; the arrows to the left indicate the contact between the posterior I3 muscle and the posterior of the radula/odontophore. The arrow to the right indicates a gap between the dorsal surface of the odontophore and the dorsal portion of the anterior I3 muscle; compare the views shown in Fig. 12D,E. (B) Dorso-ventral views of transition, protraction and retraction. The lateral groove (posteriormost edge of the 11/13/jaw complex) has been rotated so that it is vertical. (C) Antero-posterior views of transition, protraction and retraction. The left, middle and right columns are based on frames 26, 34 and 39, respectively, of bite 3213. Compare with fig. 11 of Neustadter et al. (Neustadter et al., 2002b).

maximum protraction of swallowing, the odontophore remained posterior to the line of the jaws [frame 10 of fig. 5, and fig. 11, right panels, of Neustadter et al. (Neustadter et al., 2002a)]. Furthermore, near the peak of protraction, the I2 muscle (the thin muscle that wraps around the posterior of the buccal mass, and acts to protract the odontophore [(Hurwitz et al., 1996); Fig. 1A] was shorter in biting than in swallowing [compare Fig. 3, frames 8 and 9, of this paper with fig. 5, frames 9 and 10 in Neustadter et al. (Neustadter et al., 2002a)].

During retraction, the position of the radular stalk and odontophore differed between biting and swallowing. During swallowing, the base of the radular stalk extended beyond the base of the odontophore for about a third of the entire

swallowing cycle [frames 13–20 out of the 22 frames of the swallow shown in fig. 5 in Neustadter et al. (Neustadter et al., 2002a)]. In contrast, during biting, the base of the radular stalk extended beyond the base of the odontophore for only about one-sixth of the entire biting cycle (frames 13–15 out of the 18 frames of Fig. 3). By the time the odontophore had fully rotated posteriorly, the radular stalk protruded only slightly out of the base of the odontophore, so that the characteristic  $\Gamma$  shape seen at the peak retraction of the swallowing [fig. 5, frames 18 and 19, in Neustadter et al. (Neustadter et al., 2002a)] was not observed in biting (frame 15 of Fig. 3 of this paper).

A three-dimensional model of a bite (Fig. 4), based on the kinematic model previously described (Neustadter et al.,



2002b), clearly illustrates these differences. During the initial transition phase, a larger fraction of the volume of the odontophore (yellow mesh) lies within the lumen of the I1/I3/jaw complex (blue mesh) than during the transition phase of swallowing [compare column labeled Transition in Fig. 4, with the identical column in fig. 11 of Neustadter et al. (Neustadter et al., 2002b)]. Near the peak of protraction, the anterior tip of the odontophore penetrates through the widely opened jaws, and the anterior tip of the radular stalk is closer to the anterior surface of the odontophore than it is in swallowing. The hemispherical region posterior to the I1/I3 musculature, which represents the attachment and posterior extent of the I2 muscle, is smaller in biting than in swallowing (left arrows in top frame of side view of Protraction; Fig. 4).

Fig. 5. Kinematics of the I2 muscle during biting *versus* swallowing. (A–D) Data from individual bites are shown to indicate the variability in individual responses. In all subsequent figures, only averaged data are shown. Data in A–D are plotted as length (mm) as a function of time (ms). (A) I2 kinematics in the first bite. This sequence from 7725 begins with frame 2 and ends with frame 25. The onset of the  $t_1$  period (see Materials and methods) is frame 13. (B) I2 kinematics in the second bite. This sequence from 3213 begins with frame 26 and ends with frame 43. The onset of the  $t_1$  period is frame 34. (C) I2 kinematics in the third bite. This sequence from 3213 begins with frame 43 and ends with frame 60. The onset of the  $t_1$  period is frame 49. (D) I2 kinematics in the fourth bite. This sequence from 3222 begins with frame 53 and ends with frame 72. The onset of the  $t_1$  period is frame 61. (E) Averaged data normalized to total cycle length. Lengths are not normalized. Values are means (solid lines)  $\pm$  1 s.d. (broken lines). Black lines, averaged data from biting responses; gray lines, averaged data from swallowing responses [data for swallowing in this and all subsequent figures are from Neustadter et al. (Neustadter et al., 2002a), re-analyzed using the new jaw line as described in Materials and methods]. Black vertical line represents the average  $t_4/t_1$  border for the averaged bite data; gray vertical lines represent the average  $t_4/t_1$  and  $t_1/t_2$  borders for the averaged swallow data. (F) Schematic diagrams indicating the I2 length plotted in A for frames 1, 12, 19 and 24. Muscle I2 is highlighted with a black line.

The three-dimensional model reconstruction also clearly shows that the posterior section of the I1/I3 musculature is posterior to the widest portion of the radula/odontophore, and has a narrower diameter than it did in transition [compare column labeled Protraction in Fig. 4, with the identical column in fig. 11 of Neustadter et al. (Neustadter et al., 2002b)]. Finally, the extension of the base of the radular stalk beyond the base of the odontophore is smaller than in swallowing [compare column labeled Retraction in Fig. 4, with the identical column in fig. 11 of Neustadter et al. (Neustadter et al., 2002b)].

#### Initial positions in biting versus swallowing

At the onset of biting or swallowing movements, the buccal mass is not generally at rest; rather, it is in a position that we refer to as ‘transition’. This is consistent with earlier observations in a semi-intact preparation. In that preparation, prior to the onset of rhythmic feeding-like behaviors, the entire system underwent activation that prepared it to generate feeding responses (referred to as a ‘cocking phase’) (Weiss et al., 1986).

The initial position of the radula and odontophore within the buccal mass at the time of protraction onset differed from its initial position in swallowing. In biting, the initial length of the I2 protractor muscle was significantly shorter [Fig. 5E, arrow 1; note that the error bars for biting (black) do not overlap those for swallowing (gray)]. The antero-posterior length of the ventral surface of the I1/I3/jaw complex was significantly shorter in biting (Fig. 6C, arrow 1). The dorso-ventral length of I3 at the lateral groove was significantly shorter (Fig. 6E, arrow 1), and the length of the I1/I3/jaw complex at the jaw line was significantly longer (Fig. 6G, arrow 1). The odontophore protraction into the lumen of the I1/I3/complex

allows the posterior tissue of the I1/I3/complex to shorten behind the grasper (dorso-laterally at the lateral groove), and lengthen anterior to it (dorso-laterally at the jaw). Moreover, the model suggests that the medio-lateral width is expanded at the lateral groove [top black lines in Fig. 7A–D; compare the top lines in fig. 15A–D of Neustadter et al. (Neustadter et al.,

2002b)], but of similar width at the jaws [bottom broken lines in Fig. 7A–D; compare the bottom lines in fig. 15A–D of Neustadter et al. (Neustadter et al., 2002b)]. Finally, the initial position of the tip of the odontophore is closer to the jaw line (Fig. 8C, arrow 1).

The more positive initial set point for these muscles at the

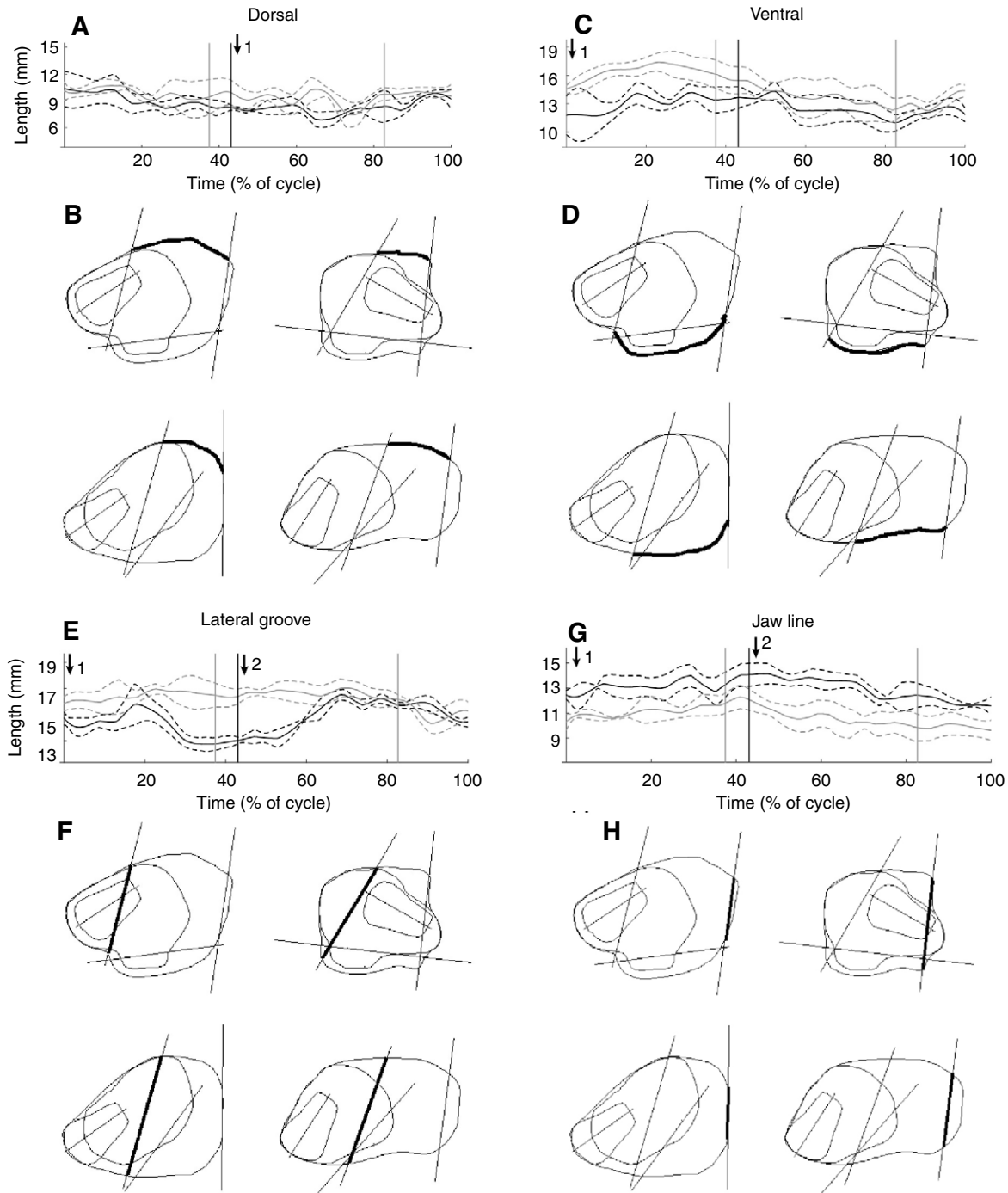


Fig. 6. Kinematics of the antero-posterior and dorso-ventral length of the I1/I3/jaw complex during biting *versus* swallowing. (A,C) Averaged antero-posterior length along the dorsal surface (A) or the ventral surface (C) during biting or swallowing, shown using black or gray lines, respectively. (E,G) Averaged dorso-ventral length at the lateral groove (E) or at the jaw line (G) during biting or swallowing, shown using black or gray lines, respectively. Values are means (solid lines)  $\pm 1$  s.d. (broken lines). (B,D,F,H) Schematic diagrams showing the lengths (bold lines) measured to generate these averages for the frames indicated in Fig. 5 through the biting cycle.

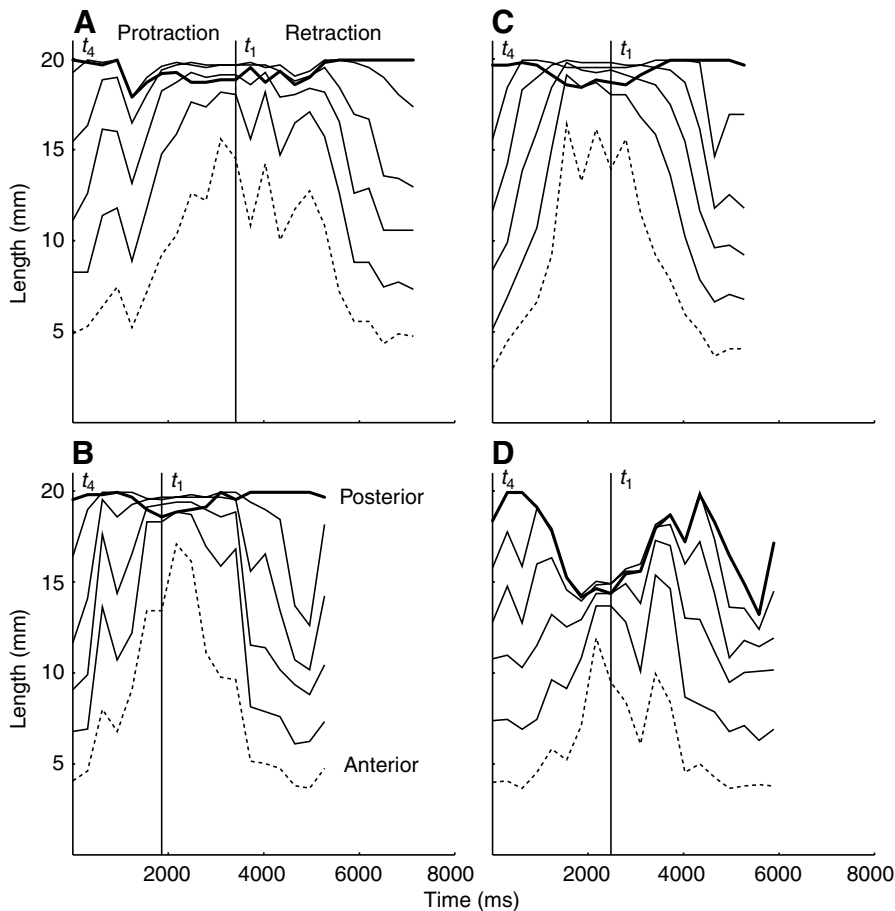


Fig. 7. Estimates of the kinematics of the medio-lateral widths of the I3 muscle during biting using the three-dimensional kinematic model. A schematic medio-lateral view of the I1/I3/jaw complex is shown in Fig. 2C. (A–D) Widths of the continuous mesh representing the I3 muscle at six evenly spaced locations along its antero-posterior length for the first to fourth bites. The top trace in each panel (solid black line) is the medio-lateral width of the I3 muscle at the lateral groove. The bottom trace in each panel (broken line) is the medio-lateral width of the I3 muscle at the jaws.

onset of biting may partially account for the short duration of the larger amplitude protraction associated with biting. Starting from a more positive position, the same total forward translation of the odontophore would reach a more positive final position in biting than in swallowing in the same period of time. However, the difference in the position of the odontophore tip at the peak protraction of biting *versus* the peak protraction of swallowing is larger than the initial difference in their positions [Fig. 8C; note that at the onset of a bite or swallow (arrow 1), the lines are separated by 2 s.d.; at the peak of protraction (arrow 2), they are separated by about 4 s.d.], so additional factors must contribute to the large protraction of biting.

#### *Odontophore shape near peak protraction in biting versus swallowing*

During biting, the grasper is protracted further anteriorly than in swallowing, inducing it to pass into the lumen of the I1/I3/jaw complex. In turn, it is possible that the forces within the I1/I3/jaw complex could deform the grasper. In response, the internal forces of the grasper might alter its shape to allow it to open and then shut prior to the peak of protraction. We therefore compared the shape of the odontophore near the peak of protraction in biting and swallowing. The antero-posterior length of the odontophore was significantly shorter near the

peak protraction of biting as compared to swallowing (Fig. 9A, arrow 1). The odontophore was significantly shorter dorso-ventrally near and after the peak of protraction in biting compared to swallowing (Fig. 9C, arrow 1), but its medio-lateral width was not significantly different (Fig. 9E). These results suggest that the overall shape of the odontophore is compressed at the peak protraction of biting in comparison to its shape during swallowing.

Biting is also associated with a larger opening of the halves of the radula. Consistent with this is the relative position of the radular stalk within the odontophore: the radular stalk is significantly further above the base of the odontophore in biting near the peak of protraction than it is during swallowing (Fig. 10C, arrow 1; Fig. 10E,F). Another indication that the radular stalk is being held tightly near the top surface of the odontophore is provided by the model estimate of the I7 muscle length: I7 is significantly shorter near the peak of protraction in biting than it is in swallowing (Fig. 11, arrow 1).

#### *I2 and I1/I3/jaw complex lengths near peak protraction in biting versus swallowing*

Do the *in vivo* kinematics support the hypothesis that I2's ability to protract may be greatly reduced, and that the posterior region of the I1/I3/complex could assist protraction? At the peak of protraction in biting, the length of the I2 muscle is

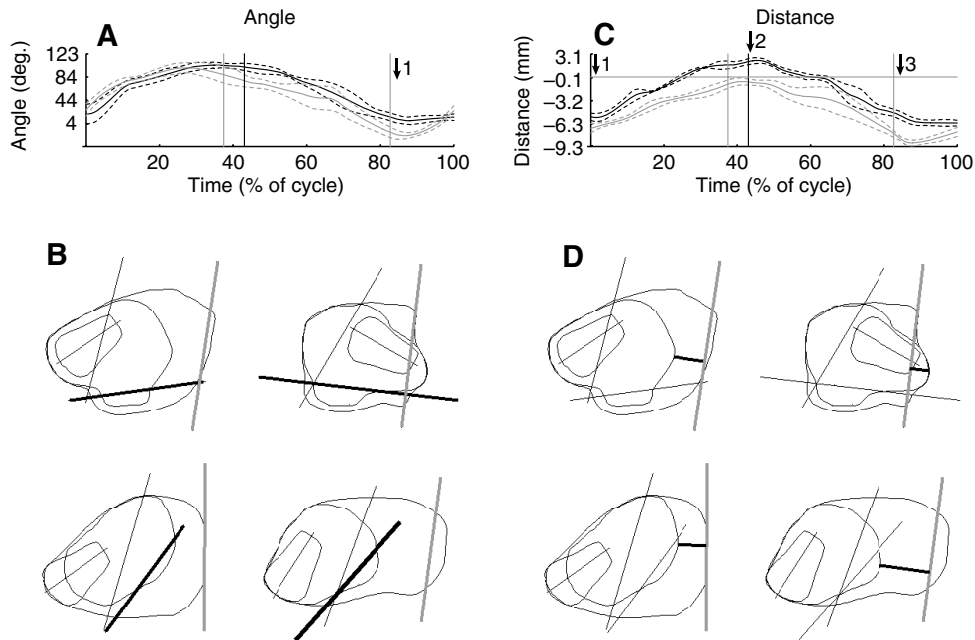


Fig. 8. Movements of the odontophore relative to the buccal mass during biting *versus* swallowing. (A) Biting (black lines) and swallowing (gray lines) data showing averaged rotation of the anterior border of the I6 relative to the jaw line (black and gray lines, respectively, in (B)). (C) Biting (black lines) and swallowing (gray lines) data showing translation of the anterior tip of the odontophore relative to the jaw line (black and gray lines, respectively, in (D)). In C, the gray horizontal line indicates the location of the jaws (corresponding to 0 mm). When the data lie above this line, the radula and underlying odontophore are protruding through the jaws. Note that the averaged swallows do not cross this line, whereas the averaged bites do cross it. Values in A and C are means (solid lines)  $\pm$  1 s.d. (broken lines).

significantly shorter than it is at the peak protraction of swallowing (Fig. 5E, arrow 2). At the peak protraction of biting, I2 is  $15.9 \pm 1.5$  mm long, whereas at the peak protraction of swallowing I2 is  $23.3 \pm 1.8$  mm long ( $P < 0.005$ ,  $N = 4$ ). The I2 muscle remains at or near its shortest length for a longer fraction of the total biting cycle than it does during the swallowing cycle (Fig. 5E). This suggests that the protractor muscle I2 is more strongly contracted during biting, consistent with the stronger activation that it receives during biting [fig. 13A,B in Hurwitz et al. (Hurwitz et al., 1996)].

Analysis of I2's length/tension and force velocity properties suggests that I2 will become weak at the peak protraction of biting. Assuming that the length of I2 at the end of the biting cycle is close to the resting length of the I2 muscle, it will be equal to  $0.86l_{\text{mto}}$  [where  $l_{\text{mto}}$  is defined as the optimal muscle and tendon length of I2 (Yu et al., 1999); note that if the longer transition length for swallowing rather than biting is used for these calculations, it will strengthen the conclusions presented]. From the actual lengths measured from the MR images, the minimum length reached by I2 prior to the peak protraction of biting is  $0.46 \pm 0.02l_{\text{mto}}$  (mean  $\pm$  s.d.,  $N = 4$ ), which is significantly shorter than the minimum length reach by I2 prior to the peak protraction of swallowing ( $0.66 \pm 0.03l_{\text{mto}}$ ;  $P < 0.0001$ ). The active forces at the minimum length that I2 reaches in the protraction of biting become close to zero [fig. 2C in Yu et al. (Yu et al., 1999)]. The ability of I2 to exert force is further reduced by its force/velocity properties. Within 200 ms of reaching its shortest length during the protraction of biting, the

I2 shortens at a velocity of  $0.18 \pm 0.09 l_{\text{mto}} s^{-1}$ , which will reduce I2's force to about 40% of the maximum it could exert isometrically [fig. 2D in Yu et al. (Yu et al., 1999)]. A kinetic model of the odontophore, I3 and I2 muscle has demonstrated that the mechanical advantage of I2 drops precipitously as it shortens (Sutton et al., 2004b). Finally, the ability of I2 to protract the radula/odontophore at the displacement associated with biting is also antagonized by both passive and active forces in the hinge, i.e. the interdigitation of the I2 muscle, the I1/I3/jaw complex and I4 (Fig. 2B1), which is stretched at the peak protraction of biting (Sutton et al., 2004a). Taken together, these data strongly suggest that other factors must contribute to the peak protraction of biting.

A kinetic model of the buccal mass predicted that the posterior part of the I1/I3/jaw complex could contribute to protraction during the peak protraction of biting (Sutton et al., 2004b). The *in vivo* kinematic data are consistent with this hypothesis. Prior to peak protraction, the posterior portion of the I1/I3/jaw complex becomes significantly shorter dorso-ventrally at the lateral groove in biting than it does in swallowing (Fig. 6E, arrow 2). At the peak protraction of biting, the length of the I3 muscle at the lateral groove is  $13.2 \pm 0.8$  mm, whereas at the peak protraction of swallowing it is  $16.3 \pm 1.1$  mm ( $P < 0.003$ ,  $N = 4$ ). This constriction is likely to be an active pinching down, because the length decreases significantly below the rest length of the muscle at the lateral groove (compare the length in Fig. 6E, arrow 1). The posterior part of the I1/I3/jaw complex also shortens medio-laterally at

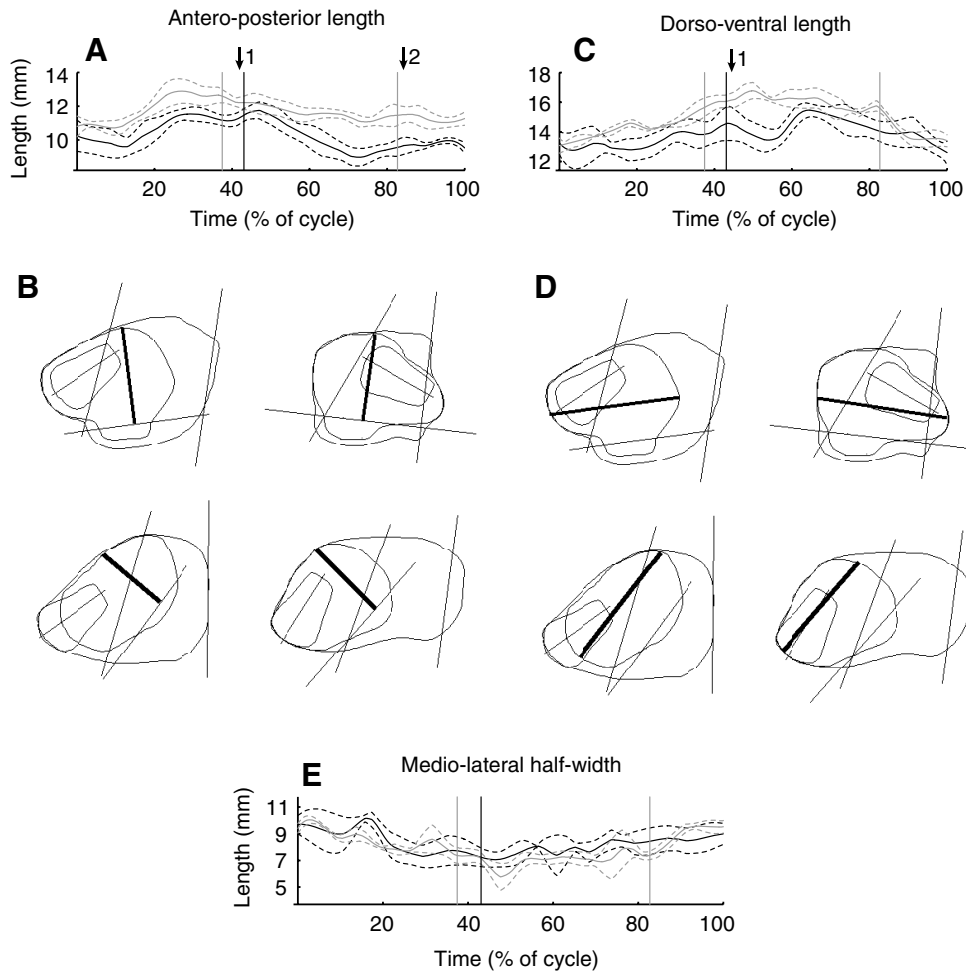


Fig. 9. Antero-posterior, dorso-ventral and medio-lateral dimensions of the odontophore during biting *versus* swallowing. Measurements were made after the anterior border of I6 had been rotated so that it was vertical. Averaged antero-posterior (A) and dorso-ventral (C) odontophore length normalized to cycle time; black lines are for biting, gray lines are for swallowing. (B,D) Schematic diagrams of lengths measured. (E) Medio-lateral half-widths in biting *versus* swallowing estimated from the kinematic model. A schematic medio-lateral view of the odontophore is shown in Fig. 2C. The half-width is reported, since this is likely to approximate the medio-lateral extent of the horseshoe-shaped I4 muscle (each half of which underlies the radula). Values in A, C and E are means (solid lines)  $\pm$  1 s.d. (broken lines).

the lateral groove (Fig. 7A–D, top thick lines, prior to  $t_1$  line marking end of protraction).

Other changes in the lengths of the I1/I3/jaw complex reflect how much further forward the grasper is protracted through the lumen of the jaws in biting than in swallowing. The antero-posterior length on the dorsal surface is shorter (Fig. 6A, arrow 1). The muscle expands dorso-ventrally (Fig. 6G, arrow 2) and medio-laterally at the jaws (Fig. 7A–D, bottom broken lines). The changes in antero-posterior length could be due both to the expansion of the entire lumen of the I1/I3/jaw complex as the grasper moves into it, and to active contraction of the I1 muscle.

#### *Differential contractile forces in the I1/I3/jaw complex*

The lengths of I2 and of the I1/I3/jaw complex prior to and at the peak of protraction support the hypothesis that the posterior section of the I1/I3/jaw complex could contribute to the protraction phase of biting. However, if the force exerted by the anterior portion of the I1/I3/jaw complex were stronger than the force exerted by the posterior region, the net force exerted by the I1/I3/jaw complex would not generate protraction. We therefore examined the anatomy of the I1/I3/jaw complex *in vitro* and *in vivo* to determine whether

there might be a difference in the forces exerted by these parts of the I1/I3/jaw complex.

The fiber directions of the I1/I3/jaw complex were visualized in formaldehyde-fixed buccal masses (Fig. 12A; lines indicate fiber directions). Contraction of the I1 muscle may shorten the antero-posterior length of the entire I1/I3/jaw complex, whereas contractions of the I3 muscle bands may constrict the entire lumen of the I1/I3/jaw complex. External fiber directions do not distinguish the anterior or posterior regions of the I1/I3/jaw complex.

The internal anatomy of the I1/I3/jaw complex does suggest differences between the anterior and posterior regions (Fig. 12C). Anteriorly, the medial surfaces of the I3 muscle bands are covered with cartilage; posteriorly, no cartilage is present. Our anatomical studies have shown that the dorsal and ventral connections of the jaw cartilages are flexible, consisting of muscle and connective tissue. Moreover, at rest, the jaw cartilage has folds in it (Fig. 12C). In freshly dissected tissue, it is possible to manually stretch these folds in a dorso-ventral direction without encountering a significant resisting force until they pull taut, after which the cartilage rigidly resists further expansion (H.J.C., unpublished observations). In contrast, the posterior region of the I3 bands generates a

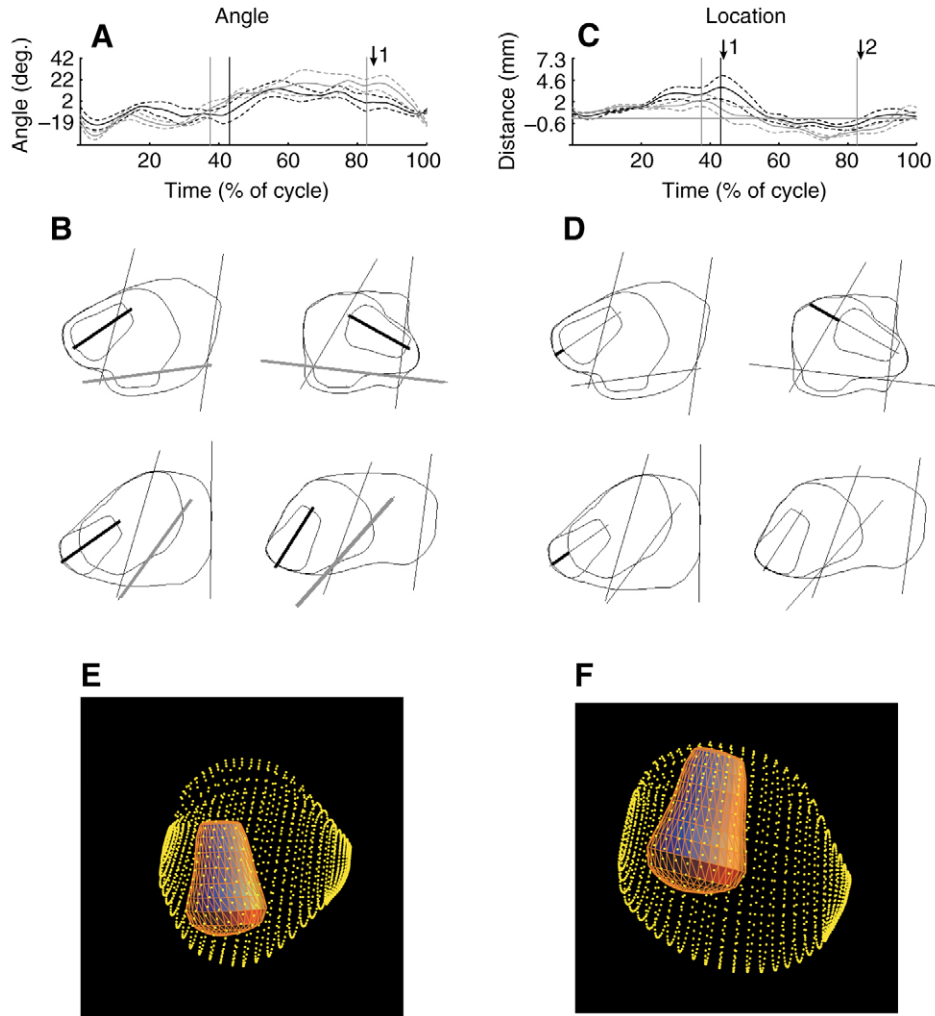


Fig. 10. Movements of the radular stalk relative to the odontophore during biting *versus* swallowing. (A–D) Averaged rotation (A) and translation (C) of the radular stalk (black lines are for biting, gray lines for swallowing). Measurements were made of the rotation of the radular stalk relative to the anterior border of muscle I6 (in B, the line of the radular stalk is highlighted with a black line, and the anterior border of muscle I6 is highlighted with a gray line), and the translation of the base of the radular stalk relative to the dorso-ventral height of the odontophore (in D, the distance from the base of the radular stalk to the base of the odontophore is highlighted with a black line). In C, the horizontal gray line indicates when the base of the radular stalk is exactly coincident with the base of the odontophore. When the data lie above this line, the radular stalk has moved towards the dorsal surface of the odontophore; when the data lie below this line, the radula stalk is protruding ventrally out of the odontophore. Values in A and C are means (solid lines)  $\pm$  1 s.d. (broken lines). (E,F) Model outputs of the peak of swallowing (E, 7732, S3, frame 26) and the peak of biting (F, 3213, S1, frame 34), to directly compare the positions of the radular stalk near the peak of protraction. The outlines of the radula/odontophore have been rotated so that the prow is straight, and lateral views are shown. Note that the radular stalk is closer to the top of the radula/odontophore at the peak protraction of biting (F) than at the peak protraction of swallowing (E).

steadily increasing resistive force to dorso-ventral expansion (presumably due to passive forces within the I3 muscle bands).

External observations of the jaws during biting suggest that the jaw cartilage does not fully expand until near the peak of protraction. We measured (1) the circumference of the jaws as they closed (Fig. 12G), (2) their circumference at the time that wrinkles appeared (indicating that the cartilage was not tightly stretched; Fig. 12F), and (3) their circumference at the peak of protraction (Fig. 12D). The ratio of the circumference at the time wrinkles were observed to the circumference at jaw closure (i.e. (2)/(1), Fig. 12F/12G) was  $1.5 \pm 0.3$ , and this

expansion in circumference is significant ( $P < 0.05$ ,  $N = 4$  bites from one animal). In contrast, the ratio of the circumference of the jaws at the peak of protraction relative to the circumference at the time wrinkles were observed (i.e. (3)/(2), Fig. 12D/12F) was  $0.97 \pm 0.1$  ( $N = 4$  bites from one animal). The circumference of the jaws at the peak of protraction was not significantly greater than the circumference of the jaws at the onset of appearance of folds, suggesting that the anterior cartilages were not stretched further at the peak of protraction.

A previous kinetic model suggested that the posterior portion of the I3 muscle could act to protract the odontophore when it

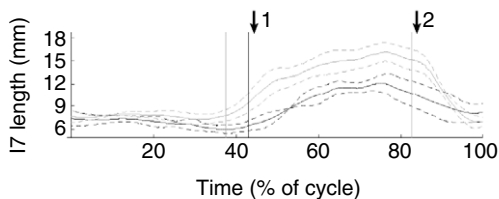


Fig. 11. Estimates of the kinematics of the I7 muscle during biting using the three-dimensional kinematic model. A schematic view of the I7 muscle during a biting cycle is shown in Fig. 2B. Averaged lengths are normalized to the cycle times; black lines are for biting, gray lines are for swallowing. Values are means (solid lines)  $\pm$  1 s.d. (broken lines).

was posterior to its midline, but the I3 muscle was represented as a torus, and the odontophore as a sphere (Sutton et al., 2004b). To estimate the net forces exerted by the I1/I3/jaw complex based on its shape and the shape of the odontophore *in vivo*, we used the meshes generated by the kinematic model (Fig. 13). The four plots in Fig. 13 indicate the total force produced by the I3 muscle at differential contraction ratios of 0.0, 0.3, 0.6 and 1.0 (from top to bottom). If the magnitude of the forces in the anterior portion of the I1/I3/jaw complex were 30% or less than the forces in the posterior portion of the I1/I3/jaw complex, it was possible for the posterior portion of the I1/I3/jaw complex to exert significant protractive forces on the odontophore prior to the peak of protraction (Fig. 13, top two lines). These results are an upper bound on the forces that the I3 muscle could exert, because they do not account for the length/tension or force/velocity properties of the I3 muscle, which are likely to reduce the forces that I3 could generate.

#### Peak retraction in biting versus swallowing

Retraction is stronger in swallowing than in biting, because the animal exerts force against food to be ingested during the retraction phase of swallowing (Hurwitz and Susswein, 1992). The halves of the radula may close together more tightly during swallowing than during biting. Shortly after peak protraction, the dorso-ventral length of the odontophore is significantly greater during swallowing than in biting (Fig. 9C, arrow 1), and remains greater during the first half of retraction. Prior to the peak of retraction, the antero-posterior length of the odontophore is significantly greater during swallowing than in biting (Fig. 9A, halfway between arrow 1 and 2). Both of these differences are consistent with tighter closure, which would expand the musculature of the odontophore in these dimensions, since the medio-lateral width is not changed significantly (Fig. 9E). Consistent with a tighter closure of the odontophore is a larger protrusion of the base of the radular stalk beyond the base of the odontophore (Fig. 10C, arrow 2), and a significantly greater increase in the estimated length of the I7 muscle (Fig. 11, between arrows 1 and 2), reflecting the greater movement of the radular stalk out of the halves of the I4 muscle.

The external forces acting on the odontophore during swallowing, which are absent during biting (because the animal

has not yet grasped anything), may also contribute to the change in shape of the odontophore. In Fig. 9C, the dorso-ventral length of the odontophore is shorter during biting than in swallowing during the first half of retraction. During this part of retraction in both biting and swallowing, the odontophore is rotated into the lumen of the I1/I3/jaw complex. As a consequence, during swallowing, the dorso-ventral dimension of the odontophore is directly in line with any opposing force due to seaweed [see Fig. 9D, top right outline, which corresponds to the onset of protraction; compare with fig. 12F, frame 18, in Neustadter et al. (Neustadter et al., 2002a)]; encountering an antagonistic force in this direction could induce expansion in this dimension during swallowing. Similarly, during late retraction in both biting and swallowing, the odontophore has rotated out of the lumen of the I1/I3/jaw complex. As a consequence, during swallowing, the antero-posterior dimension of the odontophore is directly in line with any opposing force due to seaweed [see Fig. 9B, bottom left outline, which corresponds to the peak of retraction; compare with fig. 12F, frame 18, in Neustadter et al. (Neustadter et al., 2002a)], and a force in this direction could expand the antero-posterior dimension of the odontophore during swallowing. Since an external force is absent during biting, and the odontophore does not close as tightly, the odontophore does not expand as much in either the dorso-ventral or the antero-posterior dimension during biting as it does during swallowing.

In addition to tighter closure of the odontophore halves, the overall retraction of the odontophore is greater during swallowing. The I2 muscle is longer at the peak retraction of swallowing (Fig. 5E, arrow 3), the entire odontophore moves more posteriorly (Fig. 8C, arrow 3) in swallowing than in biting, and rotates back further from the jaw line in swallowing than in biting (Fig. 8A, arrow 1). In conjunction with the tighter closure and the larger amplitude protrusion of the radular stalk beyond the base of the odontophore, the entire structure shows the  $\Gamma$  shape in swallowing, which is not observed during biting.

#### Discussion

To understand the biomechanical basis of multifunctionality, we have compared the movements of the musculature of *Aplysia's* buccal mass during biting and swallowing using magnetic resonance imaging and a kinematic model. Observation of feeding movements in intact, behaving animals demonstrated that animals made larger amplitude protractions in biting than in swallowing (Kupfermann, 1974; Morton and Chiel, 1993a). The data presented in this paper confirm these observations. Furthermore, indirect evidence suggested that the retraction phase was larger in amplitude in swallowing than in biting [(Kupfermann, 1974); fig. 5A,B in Morton and Chiel (Morton and Chiel, 1993a), showing more intense buccal nerve 2 activity, i.e. activation of the I1/I3/jaw muscle complex, during the retraction phase of swallowing than in biting]. The data presented in this paper directly demonstrate the larger amplitude of retraction movements and the tighter closing of the radula/odontophore in swallowing as compared to biting.

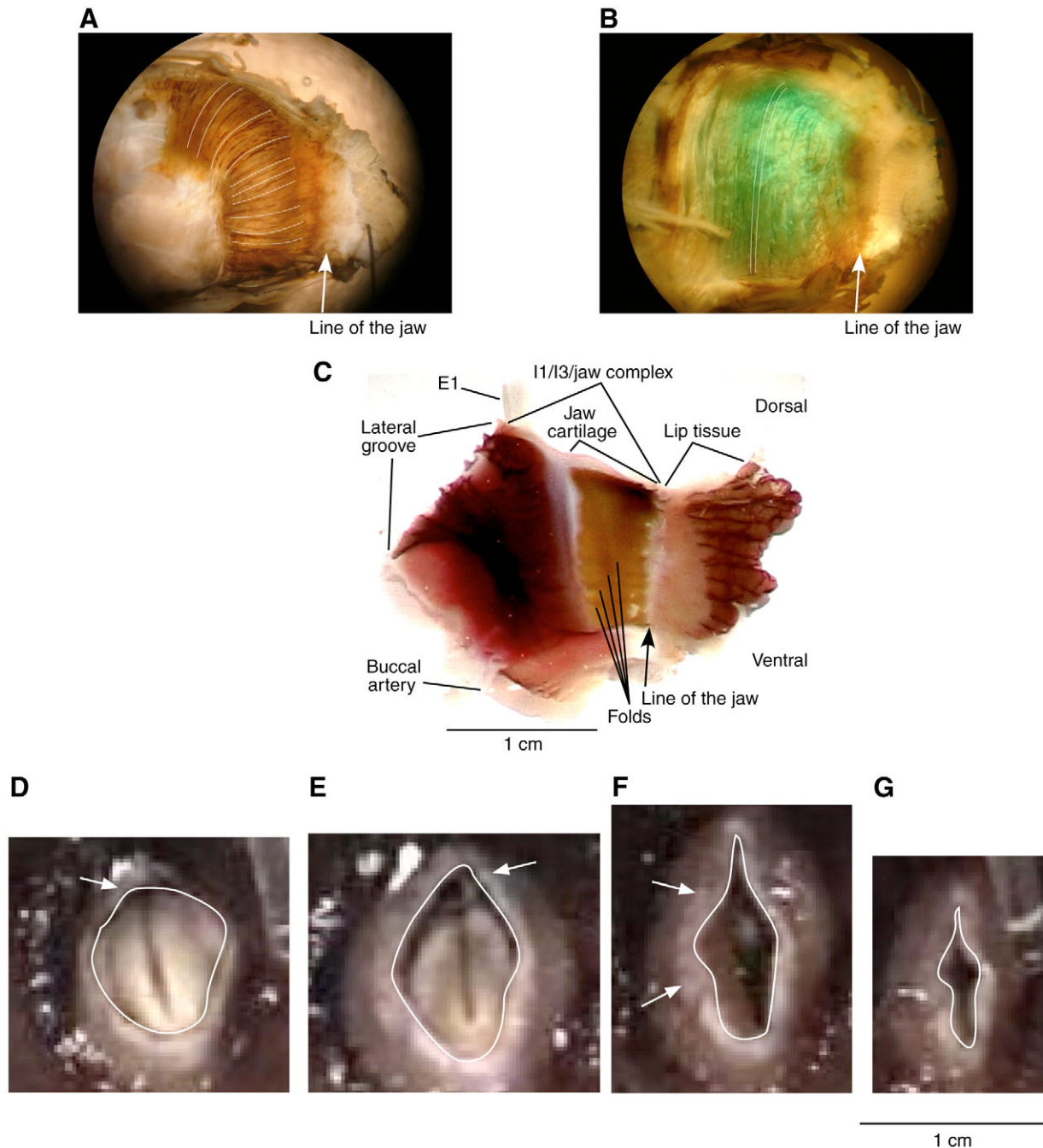
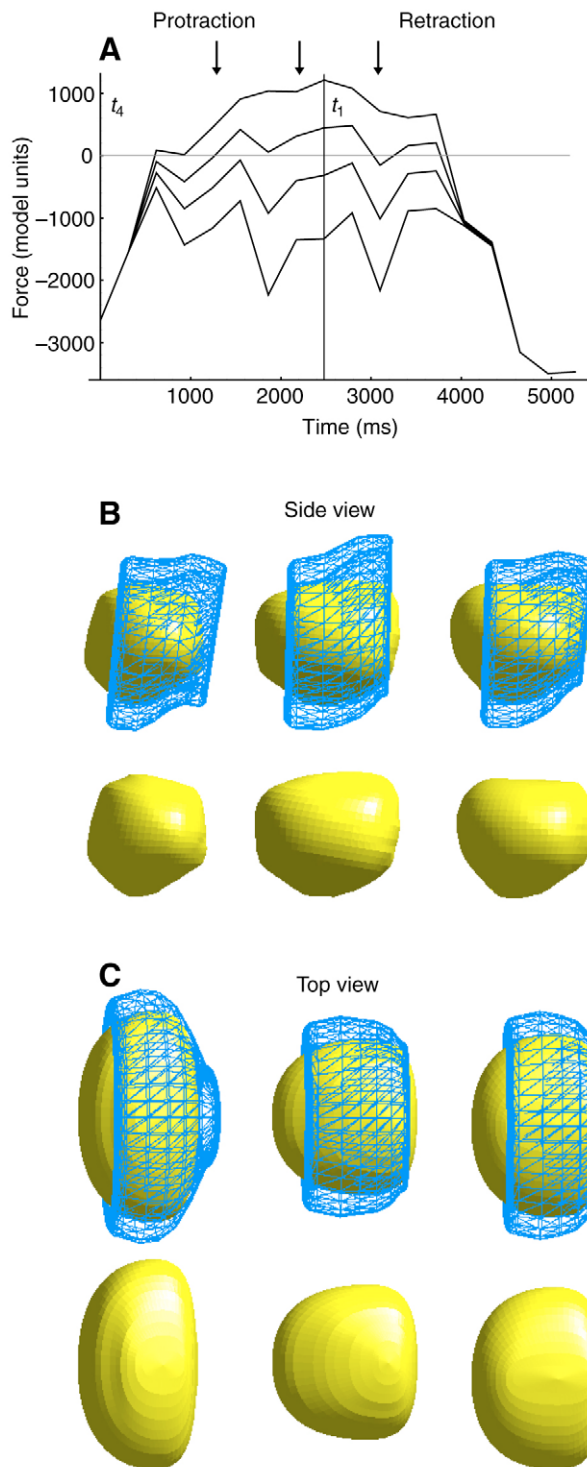


Fig. 12. External and internal anatomy of the I1/I3/jaw complex, and measurement of the circumference of the jaw cartilage during a bite. (A) Fiber directions in the I1 muscle visualized by staining with hematein (see Materials and methods). White lines have been added that closely follow discrete I1 fibers. A schematic view of fiber positions during the biting cycle is shown in Fig. 2A. (B) Fiber directions in the I3 muscle visualized by staining with Fast Green (see Materials and methods). Two white lines have been added that closely follow discrete I3 bands. (C) Dissected view of jaw cartilage within the I1/I3/jaw complex. Lines point to folds in the cartilage of the jaw. Note that the jaw cartilage only occupies approximately half of the full antero-posterior length of the I1/I3/jaw complex both dorsally and ventrally. Scale bar (1 cm) applies to A–C. (D–G) Measurement of circumference of jaw cartilage during a bite. Images are oriented so that the dorsal surface of the animal is at the top, as in Figs 1 and 2. Compare with the line drawings in fig. 2A of Morton and Chiel (Morton and Chiel, 1993a). (D) Circumference at peak protraction; the radula has just closed. Arrow indicates the dorsal region of the jaws that are not in contact with the dorsal surface of the radula. (E) Circumference just after peak protraction, as radula begins to rotate and retract posteriorly into the buccal cavity (0.5 s after image shown in D; arrow indicates the dorsal region of the jaws that is not in contact with the dorsal surface of the radula). (F) Circumference at the onset of folds in the cartilage (folds are indicated by arrows; 1.0 s after image shown in D). (G) Circumference as the jaws close (1.3 s after image shown in D).



Three novel phenomena were also observed. First, the radula/odontophore begins in a more anterior initial position at the onset of biting than at the onset of swallowing. Second, prior to and at the peak of protraction of biting, the length of the I2 muscle becomes short, and the posterior part of the I1/I3/jaw complex also shortens significantly. These observations provide kinematic support for the hypothesis that the posterior part of the I1/I3/jaw complex could contribute to

Fig. 13. Estimate of forces of I1/I3/jaw complex on odontophore. (A) Graph of estimated net forces for successive frames of sequence 3213, images 26-43. See Materials and methods for description of force calculation. Nominal model force units are plotted against time (ms). Positive force values imply that the odontophore will be protracted; negative force values imply that the odontophore will be retracted. The four lines are plotted using the assumption that the ratio of force in the anterior half to the posterior half of the I1/I3/jaw muscle complex is 0.0 (top line), 0.3 (second from top), 0.6 (third from top), or 1.0 (bottom line). Whenever the data for different force ratios lies above the zero line (as it does for ratios of 0.3 and 0.0), this indicates that the structures are kinematically configured such that with this differential excitation ratio, the I3 muscle can function as a protractor. (B) Three-dimensional model right lateral views of the I1/I3/jaw complex (blue mesh) and odontophore (yellow solid), corresponding to the arrows above A (images 31, 33 and 35, respectively). Top row: I1/I3/jaw complex and odontophore. Bottom row: odontophore alone. In the center top image, the antero-dorsal I1/I3 mesh is not in contact with the dorsal surface of the odontophore, but it is in contact with the dorsal surface of the posterior part of the odontophore. Also note that, in the central bottom image, the posterior part of the odontophore widens towards its midpoint. (C) Three-dimensional model dorso-ventral views of the I1/I3/jaw complex corresponding to the arrows above A (images 31, 33 and 35, respectively). Top row: I1/I3/jaw complex and odontophore. Bottom row: odontophore alone. In the center top image, note that the posterior I1/I3 mesh is in contact with the posterior surface of the odontophore. In the center bottom image, note that the posterior part of the odontophore widens towards its midpoint.

the peak protraction of biting. Third, the radular stalk moves close to the surface of the radula/odontophore at the peak protraction of biting, which does not occur during the peak protraction of swallowing.

#### *Context-dependent role of I1/I3/jaw complex in biting protractions*

Several lines of evidence suggest that the posterior part of the I1/I3/jaw complex may play a context-dependent role, i.e. the direction of the forces that it exerts may reverse with mechanical context. The I1/I3/jaw complex was inferred to act as a retractor from anatomical studies (Howells, 1942), and was shown to induce retraction when stimulated (Morton and Chiel, 1993a). However, near the peak protraction of biting, the I1/I3/jaw complex may also play a role in protraction. First, data from the present study demonstrate that I2 becomes short near the peak protraction of biting (Fig. 5E, arrow 2) and previous work suggests that when it is short, I2 becomes weak both because of its intrinsic length/tension and force/velocity properties [fig. 2 in Yu et al. (Yu et al., 1999)], and because I2 loses mechanical advantage, i.e. it loses the ability to convert its internal forces into forces on the odontophore [fig. 4 in Sutton et al. (Sutton et al., 2004b)]. Second, as I2 protracts the odontophore, I2 stretches the 'hinge' that connects the base of the odontophore to the surrounding muscles of the buccal mass, generating passive and active forces that antagonize the forces in I2 (Sutton et al., 2004a). Third, the position of the

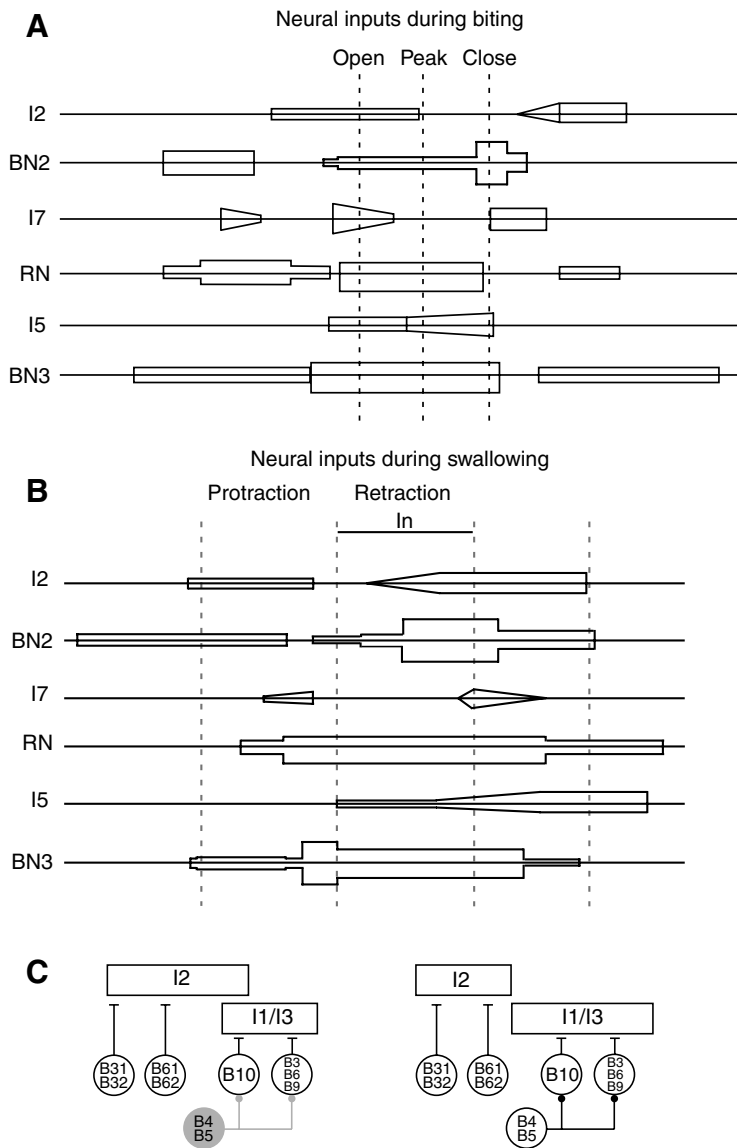


Fig. 14. (A,B) Schematic representation of neural and muscular activations during biting and swallowing cycles. Extracellular recordings from nerve and muscle in intact, behaving animals were scanned from several different sources. Simultaneous recording from BN2 and RN were taken from Morton and Chiel (Morton and Chiel, 1993a). Simultaneous recordings from BN1, BN2 and BN3 were taken from unpublished observations (D. W. Morton and H. J. Chiel). Simultaneous recordings from I2 and from BN2 were taken from Hurwitz et al. (Hurwitz et al., 1996). Extracellular recordings from I5 (ARC) were taken from Cropper et al. (Cropper et al., 1990b), and were aligned with BN3 activity (which carries the axons of the B15/B16 motor neurons). Recordings from I10 (which are representative of activity in 17, I8, I9 and I10) were taken from Evans et al. (Evans et al., 1996). The lengths of the scanned recordings were scaled relative to one another using the duration of the opening of the jaws to the closing of the jaws during a bite, and aligned by peak protraction. Boxes were then drawn around the resulting extracellular recordings, providing a schematic representation of the relative sizes of the extracellular units and their timing relative to one another. The data in the swallowing part of the figure are based on fig. 20 of Neustadter et al. (Neustadter et al., 2002b). (C) Schematic representation of roles of motor neurons and multi-action neuron B4/B5 in controlling the transition from biting to swallowing. During biting, activity in the B4/B5 neurons is reduced [(Warman and Chiel, 1995); B4/B5 are shaded]. During swallowing, activity in the B4/B5 neurons increases (Warman and Chiel, 1995), inhibiting the onset of activity in the motor neurons for the I1/I3/jaw complex, B10, B6, B3 and B9 (Gardner, 1993).

posterior portion of the I1/I3/jaw complex relative to the odontophore (Fig. 13B,C, middle column), and the significant shortening of the posterior parts of the I1/I3/jaw complex in the dorso-ventral (Fig. 6E, arrow 2) and medio-lateral (Fig. 7A–D, top thick line) dimensions could allow the posterior part of the I1/I3/complex to exert protractive forces near the peak of protraction in biting. Fourth, the internal anatomy of the I1/I3/jaw complex and external views of the jaw cartilage suggest that forces in the anterior portion of the I1/I3/jaw complex could be lower than those in the posterior portion prior to the peak of protraction (Fig. 12C–G). Fifth, calculation of the upper limits of the forces that the posterior I1/I3/jaw complex could exert on the radula/odontophore relative to the anterior part suggest that the net force in the I1/I3/jaw complex could protract the radula/odontophore near the peak protraction of biting (Fig. 13A).

Additional evidence supports the hypothesis that the posterior part of the I1/I3/jaw complex could contribute to the

peak protraction of biting. First, the initial neural input to the I1/I3/jaw complex appears to be addressed to its posterior region. Prior work has shown that the third largest unit on the nerve innervating the I1/I3/jaw complex corresponds to neuron B10 [fig. 8 in Morton and Chiel (Morton and Chiel, 1993b)], neuron B10 is active prior to other I1/I3/jaw complex neurons [fig. 6 in Morton and Chiel (Morton and Chiel, 1993b)], and neuron B10 innervates the posterior portion of the I1/I3/jaw complex (Church and Lloyd, 1994). Second, during biting, neural activation of the I2 muscle stops prior to the peak of protraction, and activity in the third largest unit innervating the I1/I3/jaw complex (presumably B10) begins before I2 has shut off. The different pattern of activity in biting and swallowing is shown schematically in Fig. 14A–C [based on fig. 11A,B in Hurwitz et al. (Hurwitz et al., 1996)]. If the I1/I3/jaw complex acted as an antagonist to the I2 muscle, it is hard to understand these observations: how could the large protractions at the peak of biting be produced by turning off activation of the sole

protractor muscle and activating its antagonist? In contrast, if the posterior part of the I1/I3/jaw complex assists the I2 muscle, as predicted by our kinetic model (Sutton et al., 2004b) and by the kinematics shown in this paper, the neural control could exploit the context dependent biomechanical properties of the posterior part of the I1/I3/jaw complex. A third line of evidence is provided by the construction of a biologically inspired gripper device consisting of concentric rings of muscle-like actuators, similar to the bands of the I3 muscle, that control a central grasper. When the central grasper was posterior to the midline of the rings, ring contraction induced a retraction of the grasper; when the central grasper was anterior to the midline of the rings, ring contraction induced a protraction of the grasper (Mangan et al., 2005).

Could neuromodulation of the I2 protractor muscle alone account for the larger amplitude protraction observed during biting? Analysis of the kinetic model suggested that if a neuromodulator increased the maximum contractile force of I2 by a factor of three, I2 might be able to act as sole protractor without assistance from the posterior region of the I1/I3/jaw complex [fig. 5 in Sutton et al. (Sutton et al., 2004b)]. Indeed, I2 is subject to neuromodulation (Hurwitz et al., 2000). Motor neurons for I2, in addition to using acetylcholine as a conventional transmitter, are also immunoreactive to myomodulin, which can act as an intrinsic neuromodulator to increase both muscle contraction amplitude and relaxation rate. Furthermore, an extrinsic neuromodulator, serotonin, can also increase muscle contraction amplitude and relaxation rate. Preliminary studies show that, at the I2 lengths observed during the peak of biting, physiological concentrations of serotonin can increase the maximum isometric force by at most a factor of two (Sutton et al., 2005). Moreover, serotonin also increases I2's rate of relaxation (as does myomodulin) (Hurwitz et al., 2000). Since I2 is turned off before the peak of protraction, neuromodulation may actually decrease the amount of force that I2 can exert at the peak protraction of biting. Thus, neuromodulation alone cannot fully account for the large amplitude protractions at the peak of biting, though it may contribute.

Several additional experiments should be done to test the hypothesis that the posterior region of the I1/I3/jaw complex contributes to the peak protraction of biting. Lesions of the posterior portion of the I1/I3/jaw complex (i.e. the region posterior to the jaw cartilage, Fig. 12C), or of its innervation, should reduce the magnitude and/or duration of the peak protraction of biting in intact, behaving animals, whereas lesions of the anterior portion of the I1/I3/jaw complex, or its innervation, should not significantly affect the peak protraction of biting. Similarly, stimulation of the posterior region of the I1/I3/jaw complex *in vitro* should generate protractive forces if the radula/odontophore is moved into the position corresponding to the peak protraction of biting, whereas the same stimulation should generate retraction if the radula/odontophore is not as strongly protracted. Preliminary results support these hypotheses (Tan et al., 2006).

If the function of the I1/I3/jaw complex depends on its

mechanical context, components of the feeding cycle cannot be defined by recording activity of identified motor neurons without regard to changes in their biomechanical function (e.g. Church and Lloyd, 1994; Murphy, 2001; Elliott and Susswein, 2002). Activity of motor neurons innervating I1/I3 may not invariably represent a 'retraction' phase, and this could alter the classification of motor phases, as well as the interpretation of the functional significance of the synaptic effects of higher order interneurons. A parallel example is provided by recent work showing that the B8 motor neuron may act as a radular closer during small amplitude swallows, but contribute to both radular closure and retraction during larger amplitude swallows (Ye et al., 2006a). Understanding the neural and mechanical mechanisms of context dependence in *Aplysia* may clarify neural control of context-dependence in mammalian and human systems (Murray et al., 1995).

#### *Neuromuscular control of biting versus swallowing*

By combining previously published data on the neural and muscular activity during biting (Cropper et al., 1990a; Cropper et al., 1990b; Morton and Chiel, 1993a; Hurwitz et al., 1996; Evans et al., 1996) (D. W. Morton and H.J.C., unpublished observations) with the kinematic data presented in this paper, it is possible to suggest hypotheses about the sequence of muscle activations that may underlie the biting cycle in contrast to the swallowing cycle (Figs 2 and 14). Because we have previously provided a detailed description of the neural activity during the swallowing cycle (Neustadter et al., 2002b), we will focus on the differences between biting and swallowing.

What differences in neural activity could account for the initial more anterior position of the entire buccal mass prior to the onset of biting as compared to swallowing? One possible mechanism could be differential activation of the extrinsic muscles that suspend the buccal mass within the head, and can move the entire structure anteriorly (Chiel et al., 1986). Indeed, *in vivo* recordings of the activity of extrinsic muscle E1, which inserts on the dorsal surface of the buccal mass at the lateral groove (see Fig. 12C) and also inserts into the anterior lip tissue (Chiel et al., 1986) (Fig. 1), demonstrate that E1 is strongly activated during the cocking phase, prior to biting, and is more strongly activated prior to a bite than to a swallow [fig. 20 in Chiel et al. (Chiel et al., 1986)]. Once the cocking phase is over, the weaker retraction movement associated with a bite may leave the musculature in a more protracted mode than after a swallow. Indeed, examining all of the kinematic measures that were different from swallowing at the onset of biting shows that they remain different at the end of the biting cycle, strongly supporting this hypothesis (Fig. 5E, Fig. 6C,E,G and Fig. 8C).

What neural activity generates the larger amplitude protraction observed during biting than during swallowing? Activity in the I2 protractor muscle is more intense and prolonged during biting than during swallowing [Fig. 14A,B, I2 schematic traces (Hurwitz et al., 1996)], which would induce a larger amplitude protraction. By pulling posteriorly on the I1/I3/jaw complex, and by translating and rotating the odontophore anteriorly, the I2 is acting not only to protract the

odontophore, but also to open the jaws. As discussed above, activation of the motor neurons for the posterior of the I1/I3/jaw complex (i.e. B10) could also allow the posterior part of this muscle complex to aid protraction [Fig. 14A,B, BN2 schematic trace, smallest amplitude unit (Sutton et al., 2004b)].

What changes in neural activity could account for the change in timing of activation of the I2 muscle and the I1/I3/jaw complex in biting as opposed to swallowing? The end of activity in the I2 muscle overlaps the onset of activity in BN2 during biting, but I2 activity ends before BN2 activity begins during swallowing (Fig. 14A,B, I2 and BN2 schematic traces; Fig. 14C). A striking feature is observed at the onset of large unit activity in swallowing that is not observed during biting: there is a burst of large units on BN3 that is absent during biting, and these large units correspond to activity in the B4/B5 neurons [fig. 8A,C in Warman and Chiel (Warman and Chiel, 1995)] (Fig. 14A,B, BN3 schematic traces; Fig. 14C). Since multiaction neurons B4/B5 strongly inhibit many of the motor neurons for the I1/I3/jaw complex (Gardner, 1993), it is possible that their increased activity in swallowing may play a role in delaying the onset of activity in the motor neuronal pool for the I1/I3/jaw muscle complex that projects through BN2 (Fig. 14C). Indeed, recent studies have shown that increased activity in the B4/B5 neurons is associated with larger delays in the onset of activity on BN2 in swallowing and rejection (Ye et al., 2006a; Ye et al., 2006b).

What changes in neural activity could account for the opening of the grasper during biting as opposed to swallowing? Several lines of evidence suggest that the I4 muscle may play a context dependent role during the peak protraction of biting. First, a large upward movement of the radular stalk may be induced by an early burst of activity in the I7 muscle [labeled 1a in fig. 4A of Evans et al. (Evans et al., 1996)], which is absent in swallowing (Fig. 14A,B, I7 traces; also note greater shortening of I7 prior to peak protraction in biting, Fig. 11, arrow 1). Second, as the radular stalk moves so that it is near the top of the odontophore (Fig. 10F), contraction of the I4 muscle could act to raise the stalk further [rather than pushing the stalk downwards, as I4 does at the peak of retraction; see fig. 19B,C in Neustadter et al. (Neustadter et al., 2002b)]. Third, prior to the peak of opening, large unit activity on the radular nerve is consistently observed (Fig. 14A, RN trace), so that I4 could actively contract to enhance the upward movement of the radular stalk.

What changes in neural activity could account for the closing of the grasper during biting as opposed to swallowing? If I4 has a context-dependent role, then the critical step for allowing the grasper to close would be pulling the radular stalk downwards within the I4, so that the I4 could then act to push the radular stalk further downwards. Interestingly, this could explain the second burst that was recorded in the I7–I10 muscles [labeled 2, in fig. 4A,B of Evans et al. (Evans et al., 1996)]. Since the recordings were performed on I10, rather than directly on I7, it is possible that this burst of activation was primarily addressed to the I8–I10 muscles, which would tend to pull the base of the radular stalk towards the base of the I4

muscle. The same neural activity might have little effect on the I7 muscle, because I7 is already short. In addition, the early activation of the I5 muscle in biting might also act to pull the radular stalk down relative to the surface of the I4 muscle (Orekhova et al., 2001). In this new configuration, the intense activation of the I4 muscle will act to push the radular stalk downwards and strongly close the grasper halves.

How is retraction initiated during biting? The initiation of retraction in biting, as well as in larger amplitude (Type B) swallows, is likely to be due to activation of the ‘hinge’, the fibers connecting the dorsal base of the grasper with the I2 muscle and the I1/I3/jaw complex. The hinge is likely to exert significant active and passive retractive forces when it is strongly stretched, as it is at the peak of biting or of large amplitude (Type B) swallows (Sutton et al., 2004a; Sutton et al., 2004b; Ye et al., 2006a). This suggests that motor neuron B7, which controls the hinge (Ye et al., 2006a), is likely to be intensely active during the retraction phase of biting. Once retraction is initiated, closure of the radular halves will induce the grasper to elongate, and net forces in the I1/I3/jaw complex will become retractive (Fig. 13) (Novakovic et al., 2006).

What changes in neural activity could account for the larger amplitude retraction in swallowing than in biting? A possible neural basis for this difference is an increase in intensity of motor neuronal activity on BN2, especially amongst the second largest and largest extracellular units on BN2 (which are likely to correspond to motor neurons B3, B6 and B9; H. Ye and H. J. Chiel, unpublished observations; Fig. 14A,B, schematic BN2 traces, largest units; Fig. 14C). These motor neurons, which innervate the medial and anterior regions of the I1/I3/jaw complex (Church and Lloyd, 1994) are likely to generate a strong contraction of the entire I1/I3/jaw complex, pushing the grasper further posteriorly than during biting. In addition, longer duration and higher frequency activity in the B8 motor neurons [reflected in the large unit activity on RN; fig. 5A,B in Morton and Chiel (Morton and Chiel, 1993a)], and higher frequency and longer duration activity in the B15/B16 motor neurons that innervate the I5 (ARC) muscle during swallowing (Cropper et al., 1990a) may also contribute to the stronger closure of the radular halves. The greater protrusion of the radular stalk generates the  $\Gamma$  shape that is observed during the peak retraction of swallowing, but not of biting (Fig. 14A,B, schematic RN and I5 traces).

#### *Implications for pattern generation in Aplysia*

These results suggest that a single pattern generator, by changing the phasing, intensity and duration of activation of similar pools of motor neuron, generates the qualitatively different ingestive behaviors of biting and swallowing. Many of the interneurons that have been suggested to play a role in switching between ingestive and egestive behaviors, as well as proprioceptors that can sense whether or not an animal has grasped food, may reorganize the pattern generator for feeding (Jing and Weiss, 2001; Jing and Weiss, 2002; Jing et al., 2004; Evans and Cropper, 1998).

The kinematic results suggest that the feeding pattern

generator must alter activity in several motor neuronal groups. First, activation duration of the I2 motor neurons should increase during biting to increase protraction amplitude. Second, the intensity of activity of the B4/B5 multiaction neurons should decrease during biting to allow motor neurons for the I1/I3/jaw complex to turn on before the end of activity in the I2 motor neurons (Fig. 14C). Third, I7 should be activated early in biting to induce strong opening. Finally, motor neurons for the I1/I3/jaw complex should be more intensely activated during swallowing to increase retraction amplitude.

The duration of activity in the I2 protractor muscle could be controlled in several ways. The B31/B32 neurons, which are half of I2's motor pool for the I2 muscle (the other motor neurons are B61 and B62), are also interneurons whose activity triggers the initiation and the protraction phase of all feeding responses (Hurwitz et al., 1996). Control of the activation duration of the B31/B32 neurons would therefore control the duration of I2's excitation. Two neurons that could control B31/B32 activation duration are B63 and B64 (Hurwitz et al., 1997). Activation of neuron B63 could enhance activity in the B31/B32 neurons, since B63 is tightly coupled to the B31/B32 neurons, but has a lower threshold for excitation, and is a synaptic target for B50 (Dembrow et al., 2003; Dembrow et al., 2004) and higher order interneurons (Hurwitz et al., 2003). Increasing the excitation of B63 has been shown to initiate and prolong activity in the B31/B32 neurons (Hurwitz et al., 2003; Dembrow et al., 2004). In contrast, activity in the B31/B32 neurons can be reduced through the actions of neuron B64, which strongly hyperpolarizes the B31/B32 neurons, and contributes to the termination of protraction (Hurwitz and Susswein, 1996). Thus, neurons that hyperpolarize B64 could prolong protraction (Jing et al., 2003).

Prolonging the duration of activity in the I2 protractor muscle alone is not enough to generate biting *versus* swallowing. A recent study (Ye et al., 2006a) demonstrated that *Aplysia* can generate smaller amplitude (Type A) or larger amplitude (Type B) swallows, and that Type B swallows are associated with a significant increase in activation duration of the I2 muscle [figs 11A, 12A in Ye et al. (Ye et al., 2006a)]. The key neural difference between both types of swallows and biting is the level of activity in the B4/B5 multiaction neurons, which show little or no activity during biting, and more intense activity during swallowing (Warman and Chiel, 1995), with the most intense activity associated with the swallow that has the larger amplitude protraction (Ye et al., 2006a). Thus, recent *in vitro* studies that distinguished biting-like and swallowing-like patterns based primarily on the duration of activity in the I2 motor neurons (Jing et al., 2004) may not have accurately associated these patterns with corresponding *in vivo* behaviors.

#### *Implications for multifunctionality*

What implications do these results have for understanding multifunctionality? By design, an engineered device has a clearly defined function by which it can be evaluated. A hammer whose head breaks off as it is being used to pound

nails into a board is either worn out or poorly designed. Each component of a multifunctional engineered device, such as a Swiss Army knife, can be evaluated by focusing on each function. Thus, a Swiss Army knife may function well as a knife, but its scissors may be small and cut poorly.

How should functions of an evolved system be defined and evaluated? From an evolutionary standpoint, the only 'evaluation' that matters is whether an animal survives long enough to leave offspring, and whether it leaves more offspring than other animals in the population. Thus, it would be reasonable to define 'function' in terms of survival and reproduction. From this viewpoint, the three feeding responses in *Aplysia*, i.e. biting, swallowing and rejection, are all aspects of the single behavior of feeding, since rejection clears the buccal cavity so that animals may again attempt to ingest food (Katzoff et al., 2006). In contrast, egg laying, although it also uses the anterior tentacles and lips of the animals (Begnoche et al., 1996), clearly serves a distinctive reproductive function.

Defining function is not a purely semantic exercise. If biting, swallowing and rejection all serve a single behavioral function, i.e. feeding, neural control that can flexibly switch among the different behavioral responses may confer a selective advantage on an animal. At the same time, neural control that shuts down one set of behaviors when incompatible behaviors are to be performed by the same peripheral structures may also confer a selective advantage. Indeed, in *Aplysia*, egg-laying hormone not only induces egg laying movements of the feeding apparatus, but also suppresses the animal's own feeding responses (Stuart and Strumwasser, 1980), thus preventing an *Aplysia* from eating its own eggs and blocking its own reproduction. Similarly, *Clione*'s slow swimming movements are completely inhibited by defensive withdrawal behaviors, during which its wings are strongly retracted (Norekian and Satterlie, 1996). Under these conditions, neural control may directly instantiate behavioral hierarchies [(Tinbergen, 1951), pp. 102-104].

Alternatively, function can be defined purely by biomechanical constraints (Stein et al., 1986). Since it is not possible to locomote forwards and backwards simultaneously, these behaviors may be distinct. Since an animal cannot ingest food and reject it simultaneously, swallowing and rejection may be distinct. Similarly, since it is not possible to attempt to grasp food (i.e. bite) and to have succeeded in grasping the food and ingesting it (i.e. swallow) simultaneously, biting and swallowing may be distinct. However, functional distinctions due to biomechanics may not be strongly distinguished in neural control, if the different movements are all components of the same overall behavior. Indeed, previous studies have described intermediate motor patterns that combine features of both swallowing and rejection (Morton and Chiel, 1993a), and have also described bite/swallows: an animal begins with a bite (i.e. generates a large amplitude protraction) but, as it grasps food, completes the behavior as a swallow [i.e. generates a large amplitude retraction (Weiss et al., 1986)].

Functional differences among distinct and incompatible behaviors may affect neural control in other systems. For

example, red-eared slider turtles (*Trachemys scripta elegans*) use both forward and backward swimming and claw vibration as part of courtship (Cagle, 1950). Thus, it is not surprising that the detailed studies of Stein, Berkowitz, and their colleagues have found, at the motor pattern level, blends (i.e. switches between behaviors for several cycles, or aspects of different behaviors in successive cycles) that lead to rapid transitions among these behaviors, and, at the neural level, shared neural circuitry controlling these motor tasks (Stein, 2005; Berkowitz, 2001; Berkowitz, 2002; Berkowitz, 2005). Since limb withdrawal into the carapace is a defensive withdrawal response, it is also not surprising that neural control, and even specialized musculature, may differ for this behavior (Callister et al., 1992; Callister and Peterson, 1992).

Multifunctionality is a ubiquitous feature of many biological organisms. The ability to rapidly reconfigure a peripheral structure, flexibly adjusting motor responses as the environment changes, may confer selective advantages on animals. Motor control is likely to exploit the fluidity of peripheral function during related responses that subserve a single behavior such as feeding (Ye et al., 2006b). In contrast, when behaviors such as feeding, reproduction or escape are in conflict, neural control may act to suppress one function and enhance another. These principles are likely to be relevant to the analysis of multifunctionality in other animals and humans.

#### List of abbreviations

MR	magnetic resonance
MRI	magnetic resonance imaging
RSW	radular stalk width
$l_{\text{mto}}$	optimal muscle and tendon length
BN1	buccal nerve 1
BN2	buccal nerve 2
BN3	buccal nerve 3
ARC	accessory radula closer muscle

We thank the Whitehall Foundation (grant M97-12 to H.J.C.), the National Science Foundation (grants IBN-9974394 and IBN-0218386 to H.J.C.), and the National Institutes of Health (grant NS-047073 to H.J.C.) for supporting this research. We thank the MR Systems Department, G. E. Medical Systems Israel Ltd, Tirat Carmel, Israel, for providing us access to the magnetic resonance equipment for performing these studies. We thank Dr Greg Sutton for helpful suggestions for estimating the forces exerted by the I1/I3/jaw complex on the odontophore and for valuable comments on an earlier draft of the manuscript. We also thank Dr Hui Ye and two anonymous reviewers for their helpful comments on earlier drafts of the manuscript.

#### References

- Ashley-Ross, M. A. and Lauder, G. V. (1997). Motor patterns and kinematics during backward walking in the Pacific Giant Salamander: evidence for novel motor output. *J. Neurophysiol.* **78**, 3047-3060.
- Begnoche, V. L., Moore, S. K., Blum, N., Van Gils, C. and Mayeri, E. (1996). Sign stimulus activates a peptidergic neural system controlling reproductive behavior in *Aplysia*. *J. Neurophysiol.* **75**, 2161-2166.
- Berkowitz, A. (2001). Broadly tuned spinal neurons for each form of fictive scratching in spinal turtles. *J. Neurophysiol.* **86**, 1017-1025.
- Berkowitz, A. (2002). Both shared and specialized spinal circuitry for scratching and swimming in turtles. *J. Comp. Physiol. A* **188**, 225-234.
- Berkowitz, A. (2005). Physiology and morphology indicate that individual spinal interneurons contribute to diverse limb movements. *J. Neurophysiol.* **94**, 4455-4470.
- Biewener, A. A. (2002). Future directions for the analysis of musculoskeletal design and locomotor performance. *J. Morphol.* **252**, 38-51.
- Büschges, A. (2005). Sensory control and organization for neural networks mediating coordination of multisegmental organs for locomotion. *J. Neurophysiol.* **93**, 1127-1135.
- Cagle, F. R. (1950). The life history of the Slider turtle, *Pseudemys scripta troostii* (Holbrook). *Ecol. Monogr.* **20**, 31-54.
- Callister, R. J. and Peterson, E. H. (1992). Design and control of the head retractor muscle in a turtle, *Pseudemys (trachemys) scripta*: II. Efferent innervation. *J. Comp. Neurol.* **325**, 422-434.
- Callister, R. J., Callister, R. and Peterson, E. H. (1992). Design and control of the head retractor muscle in a turtle, *Pseudemys (trachemys) scripta*: I. Architecture and histochemistry of single muscle fibers. *J. Comp. Neurol.* **325**, 405-421.
- Chiel, H. J., Weiss, K. R. and Kupfermann, I. (1986). An identified histaminergic neuron modulates feeding motor circuitry in *Aplysia*. *J. Neurosci.* **6**, 2427-2450.
- Church, P. J. and Lloyd, P. E. (1994). Activity of multiple identified motor neurons recorded intracellularly during evoked feeding like motor programs in *Aplysia*. *J. Neurophysiol.* **72**, 1794-1809.
- Cropper, E. C., Kupfermann, I. and Weiss, K. R. (1990a). Differential firing patterns of the peptide-containing cholinergic motor neurons B15 and B16 during feeding behavior in *Aplysia*. *Br. Res.* **522**, 176-179.
- Cropper, E. C., Price, D., Tenenbaum, R., Kupfermann, I. and Weiss, K. R. (1990b). Release of peptide cotransmitters from a cholinergic motor neuron under physiological conditions. *Proc. Natl. Acad. Sci. USA* **87**, 933-937.
- Dembrow, N. C., Jing, J., Proekt, A., Romero, A., Vilim, F. S., Cropper, E. C. and Weiss, K. R. (2003). A newly identified buccal interneuron initiates and modulates feeding motor programs in *Aplysia*. *J. Neurophysiol.* **90**, 2190-2204.
- Dembrow, N. C., Jing, J., Brezina, V. and Weiss, K. R. (2004). A specific synaptic pathway activates a conditional plateau potential underlying protraction phase in the *Aplysia* feeding central pattern generator. *J. Neurosci.* **24**, 5230-5238.
- Drushel, R. F., Neustadter, D. M., Shallenberger, L. L., Crago, P. E. and Chiel, H. J. (1997). The kinematics of swallowing in the buccal mass of *Aplysia californica*. *J. Exp. Biol.* **200**, 735-752.
- Drushel, R. F., Neustadter, D. M., Hurwitz, I., Crago, P. E. and Chiel, H. J. (1998). Kinematic models of the buccal mass of *Aplysia*. *J. Exp. Biol.* **201**, 1563-1583.
- Earhart, G. M. and Stein, P. S. G. (2000). Step, swim and scratch motor patterns in the turtle. *J. Neurophysiol.* **84**, 2181-2190.
- Elliott, C. J. H. and Susswein, A. J. (2002). Comparative neuroethology of feeding control in mollusks. *J. Exp. Biol.* **205**, 877-896.
- Evans, C. G. and Cropper, E. C. (1998). Proprioceptive input to feeding motor programs in *Aplysia*. *J. Neurosci.* **18**, 8016-8031.
- Evans, C. G., Rosen, S., Kupfermann, I., Weiss, K. R. and Cropper, E. C. (1996). Characterization of a radula opener neuromuscular system in *Aplysia*. *J. Neurophysiol.* **76**, 1267-1281.
- Gardner, D. (1993). Static determinants of synaptic strength. In *The Neurobiology of Neural Networks* (ed. D. Gardner), pp. 21-70. Cambridge, MA: MIT Press.
- Gestreau, C., Dutschmann, M., Obled, S. and Bianchi, A. L. (2005). Activation of XII motoneurons and premotor neurons during various oropharyngeal behaviors. *Respir. Physiol. Neurobiol.* **147**, 159-176.
- Harris-Warrick, R. M., Marder, E., Selverston, A. I. and Moulins, M. (1992). *Dynamic Biological Networks: The Stomatogastric Nervous System*. Cambridge, MA: MIT Press.
- Howells, H. H. (1942). The structure and function of the alimentary canal of *Aplysia punctata*. *Q. J. Microsc. Sci.* **83**, 357-397.
- Hurwitz, I. and Susswein, A. J. (1992). Adaptation of feeding sequences in *Aplysia oculifera* to changes in the load and width of food. *J. Exp. Biol.* **166**, 215-235.
- Hurwitz, I. and Susswein, A. J. (1996). B64, a newly identified central pattern

- generator element producing a phase switch from protraction to retraction in buccal motor programs of *Aplysia californica*. *J. Neurophysiol.* **75**, 1327-1344.
- Hurwitz, I., Neustadter, D. M., Morton, D. W., Chiel, H. J. and Susswein, A. J.** (1996). Activity patterns of the B31/B32 pattern initiators innervating the I2 muscle of the buccal mass during normal feeding movements in *Aplysia californica*. *J. Neurophysiol.* **75**, 1309-1326.
- Hurwitz, I., Kupfermann, I. and Susswein, A. J.** (1997). Different roles of neurons B63 and B34 that are active during the protraction phase of buccal motor programs in *Aplysia californica*. *J. Neurophysiol.* **75**, 1327-1344.
- Hurwitz, I., Cropper, E. C., Vilim, F. S., Alexeeva, V., Susswein, A. J., Kupfermann, I. and Weiss, K. R.** (2000). Serotonergic and peptidergic modulation of the buccal mass protractor muscle (I2) in *Aplysia*. *J. Neurophysiol.* **84**, 2810-2820.
- Hurwitz, I., Kupfermann, I. and Weiss, K. R.** (2003). Fast synaptic connections from CBIs to pattern-generating neurons in *Aplysia*: Initiation and modification of motor programs. *J. Neurophysiol.* **89**, 2120-2136.
- Jing, J. and Weiss, K. R.** (2001). Neural mechanisms of motor program switching in *Aplysia*. *J. Neurosci.* **21**, 7349-7362.
- Jing, J. and Weiss, K. R.** (2002). Interneuronal basis of the generation of related but distinct motor programs in *Aplysia*: implications for current neuronal models of vertebrate intralimb coordination. *J. Neurosci.* **22**, 6228-6238.
- Jing, J., Vilim, F. S., Wu, J. S., Park, J. H. and Weiss, K. R.** (2003). Concerted GABAergic actions of *Aplysia* feeding interneurons in motor program specification. *J. Neurosci.* **23**, 5283-5294.
- Jing, J., Cropper, E. C., Hurwitz, I. and Weiss, K. R.** (2004). The construction of movement with behavior-specific and behavior-independent modules. *J. Neurosci.* **24**, 6315-6325.
- Katzoff, A., Ben-Gedalya, T., Hurwitz, I., Miller, N., Susswein, Y. Z. and Susswein, A. J.** (2006). Nitric oxide signals that *Aplysia* have attempted to eat, a necessary component of memory formation after learning that food is inedible. *J. Neurophysiol.* **96**, 1247-1257.
- Kelso, J. A. S.** (1995). *Dynamic Patterns*. Cambridge, MA: MIT Press.
- Kier, W. M. and Smith, K. K.** (1985). Tongues, tentacles, and trunks: the biomechanics of movement in muscular-hydrostats. *Zool. J. Linn. Soc.* **83**, 307-324.
- Kupfermann, I.** (1974). Feeding behavior in *Aplysia*: a simple system for the study of motivation. *Behav. Biol.* **10**, 1-26.
- Mangan, E. V., Kingsley, D. A., Quinn, R. D., Sutton, G. P., Mansour, J. M. and Chiel, H. J.** (2005). A biologically inspired gripping device. *Ind. Rob.* **32**, 49-54.
- Mortin, L. I., Keifer, J. and Stein, P. S. G.** (1985). Three forms of the scratch reflex in the spinal turtle: movement analyses. *J. Neurophysiol.* **53**, 1501-1516.
- Morton, D. W. and Chiel, H. J.** (1993a). *In vivo* buccal nerve activity that distinguishes ingestion from rejection can be used to predict behavioral transitions in *Aplysia*. *J. Comp. Physiol. A* **172**, 17-32.
- Morton, D. W. and Chiel, H. J.** (1993b). The timing of activity in motor neurons that produce radula movements distinguishes ingestion-like and rejection-like motor patterns in a reduced preparation of *Aplysia*. *J. Comp. Physiol. A* **173**, 519-536.
- Morton, D. W. and Chiel, H. J.** (1994). Neural architectures for adaptive behavior. *Trends Neurosci.* **17**, 413-420.
- Murphy, A. D.** (2001). The neuronal basis of feeding in the snail *Helisoma*, with comparisons to selected gastropods. *Prog. Neurobiol.* **63**, 383-408.
- Murray, W. M., Delp, S. L. and Buchanan, T. S.** (1995). Variation of muscle moment arms with elbow and forearm position. *J. Biomech.* **28**, 513-525.
- Neustadter, D. M. and Chiel, H. J.** (2004). Imaging freely moving subjects using continuous interleaved orthogonal magnetic resonance imaging. *Magn. Reson. Imaging* **22**, 329-343.
- Neustadter, D. M., Drushel, R. F. and Chiel, H. J.** (2002a). Kinematics of the buccal mass during swallowing based on magnetic resonance imaging in intact, behaving *Aplysia californica*. *J. Exp. Biol.* **205**, 939-958.
- Neustadter, D. M., Drushel, R. F., Crago, P. E., Adams, B. W. and Chiel, H. J.** (2002b). A kinematic model of swallowing in *Aplysia californica* based on radula/odontophore kinematics and *in vivo* magnetic resonance images. *J. Exp. Biol.* **205**, 3177-3206.
- Norekian, T. P. and Satterlie, R. A.** (1996). Whole body withdrawal circuit and its involvement in the behavioral hierarchy of the mollusk *Clione limacine*. *J. Neurophysiol.* **75**, 529-537.
- Novakovic, V., Sutton, G. P., Neustadter, D. M., Beer, R. D. and Chiel, H. J.** (2006). Mechanical reconfiguration mediates swallowing and rejection in *Aplysia californica*. *J. Comp. Physiol. A* **192**, 857-870.
- Orehova, I. V., Jing, J., Brezina, V., DiCaprio, R. A., Weiss, K. R. and Cropper, E. C.** (2001). Sonometric measurements of motor-neuron-evoked movements of an internal feeding structure (the radula) in *Aplysia*. *J. Neurophysiol.* **86**, 1057-1061.
- Starmühlner, F.** (1956). Beiträge zur Mikroanatomie und Histologie des Darmkanals einiger Opisthobranchier. I. *Sitzungsberichte d. Math. Naturw. Kl. Abt. I* **165**, 8-152.
- Stein, P. S. G.** (2005). Neuronal control of turtle hindlimb motor rhythms. *J. Comp. Physiol. A* **191**, 213-229.
- Stein, P. S. G., Mortin, L. I. and Robertson, G. A.** (1986). The forms of a task and their blends. In *Neurobiology of Vertebrate Locomotion* (ed. S. Grillner, P. S. G. Stein, D. G. Stuart, H. Forsberg and R. M. Herman), pp. 201-216. London: Macmillan.
- Stuart, D. K. and Strumwasser, F.** (1980). Neuronal sites of action of a neurosecretory peptide, egg-laying hormone, in *Aplysia californica*. *J. Neurophysiol.* **43**, 499-519.
- Sutton, G. P., Mackinn, J. B., Gartman, S. S., Sunny, G. P., Beer, R. D., Crago, P. E., Neustadter, D. M. and Chiel, H. J.** (2004a). Passive hinge forces in the feeding apparatus of *Aplysia* aid retraction during biting but not during swallowing. *J. Comp. Physiol. A* **190**, 501-514.
- Sutton, G. P., Mangan, E. V., Neustadter, D. M., Beer, R. D., Crago, P. E. and Chiel, H. J.** (2004b). Neural control exploits changing mechanical advantage and context dependence to generate different feeding responses in *Aplysia*. *Biol. Cybern.* **91**, 333-345.
- Sutton, G. P., Higashikubo, B. T., Lu, H. and Chiel, H. J.** (2005). Serotonergic neuromodulation contributes to the peak protraction of biting in *Aplysia californica*. Program No. 752.7. 2005 Abstract Viewer/Itinerary Planner. Washington, DC: Society for Neuroscience.
- Tan, J. T., McManus, J. M., Yungster, Y. and Chiel, H. J.** (2006). Biomechanical and neural evidence for the context dependence of the I1/I3 muscle in *Aplysia californica*. Program 253.21. 2006 Neuroscience Meeting Planner. Atlanta, GA: Society for Neuroscience.
- Tinbergen, N.** (1951). *The Study of Instinct*. Oxford: Oxford University Press.
- Ting, L. H., Kautz, S. A., Brown, D. A. and Zajac, F. E.** (1999). Phase reversal of biomechanical functions and muscle activity in backward pedaling. *J. Neurophysiol.* **81**, 544-551.
- van Leeuwen, J. L., De Groot, J. H. and Kier, W. M.** (2000). Evolutionary mechanics of protrusible tentacles and tongues. *Neth. J. Zool.* **50**, 113-139.
- Warman, E. N. and Chiel, H. J.** (1995). A new technique for chronic single-unit extracellular recording in freely behaving animals using pipette electrodes. *J. Neurosci. Methods* **57**, 161-169.
- Weiss, K. R., Chiel, H. J., Koch, U. and Kupfermann, I.** (1986). Activity of an identified histaminergic neuron, and its possible role in arousal of feeding behavior in semi-intact *Aplysia*. *J. Neurosci.* **6**, 2403-2415.
- Ye, H., Morton, D. W. and Chiel, H. J.** (2006a). Neuromechanics of coordination during swallowing in *Aplysia californica*. *J. Neurosci.* **26**, 1470-1485.
- Ye, H., Morton, D. W. and Chiel, H. J.** (2006b). Neuromechanics of multifunctionality during rejection in *Aplysia californica*. *J. Neurosci.* **26**, 10743-10755.
- Yu, S.-N., Crago, P. E. and Chiel, H. J.** (1999). Biomechanical properties and a kinetic simulation model of the smooth muscle I2 in the buccal mass of *Aplysia*. *Biol. Cybern.* **81**, 505-513.